POLITECNICO
MILANO 1863

SCUOLA DI INGEGNERIA INDUSTRIALE
E DELL'INFORMAZIONE

Heat Transfer in Compact Plate Steam Generators

TESI DI LAUREA MAGISTRALE IN
NUCLEAR ENGINEERING
INGEGNERIA NUCLEARE

Author: **Alessandro Passerin d'Entreves**

Student ID: 10526992
Advisor: Marco Enrico Ricotti
Co-advisor: Stefano Lorenzi
Academic Year: 2022-23

Towards European Licensing of Small Modular Reactors

Abstract

More than ever in recent years, nuclear energy has become the centre of public attention. Nuclear energy is a practical solution in response to a global push by first world countries to limit their CO_2 emissions and by developing countries to grow their economies without depending on fossil fuels. The low CO_2 output, low LCOE, and reliability in supplying a steady source of energy are just a few of the many benefits.

Initial cost, however, continues to be a significant obstacle, particularly for underdeveloped nations. The Small Modular Reactors (SMRs) fill this void. They are, in essence, more compact, affordable, simple to construct, and easier to maintain than large reactors (LRs). Research and experimentation, particularly in the area of safety assessment, are essential to ensuring the growth and success of this technology. Light water reactors (LWRs), which have been the most developed form of design since the 1960s, are a foundation for many SMR designs. Just scaling large reactors' major components like pumps, steam generators, pressurizers, etc. is insufficient. Current and emerging technologies need to be thoroughly studied and tested.

An essential part of LWRs is a steam generator, which transfers power from the primary loop (attached to the reactor) to the secondary loop (connected to the turbines). By analysing the performance of a compact plate heat exchanger (PHE) employed as a steam generator as part of the heat removal system of a SMR under the ELSMOR project, this thesis will attempt to close a gap in that effort. Understanding such component will help the further development and proliferation of SMRs.

After a brief overlook on SMRs and the ELSMOR's facility, an analysis of the compact plate heat exchanger working with liquid-liquid and liquid-evaporating fluids is performed. The most common heat transfer correlations in literature are presented and validated on the experimental data gathered during SIET test campaign and then compared with the heat transfer coefficient extracted by the raw data. Afterward an ad hoc heat transfer correlation is modelled in order to achieve a better fit with the experimental results.

Key-words: heat transfer coefficient, compact plate heat exchanger, SMR, ELSMOR

Abstract in italiano

Recentemente, l'energia nucleare è al centro di un acceso dibattito pubblico. L'energia nucleare è una delle soluzioni dei paesi del primo mondo per limitare le loro emissioni di CO_2 e dei paesi in via di sviluppo che vogliono far crescere le loro economie senza dover dipendere dai combustibili fossili. La bassa emissione di CO_2, il basso LCOE e l'affidabilità nella fornitura di energia costante sono solo alcuni dei numerosi vantaggi.

Il costo iniziale, tuttavia, continua ad essere un ostacolo significativo, in particolare per le nazioni sottosviluppate. Gli Small Modular Reactors (SMR) soddisfano questa richiesta. Sono, in sostanza, più compatti, economici, semplici da costruire e più facili da mantenere rispetto ai grandi reattori. La ricerca e la sperimentazione, in particolare nell'ambito dei sistemi di sicurezza, sono essenziali per garantire la crescita e il successo di questa tecnologia. I reattori ad acqua leggera (LWR), che sono stati la forma più sviluppata dagli anni '60, sono una base per molti design di SMR odierni. Il solo ridimensionamento dei componenti principali dei grandi reattori come pompe, generatori di vapore, pressurizzatori, ecc. non è sufficiente. Le tecnologie attuali ed emergenti devono essere studiate e testate a fondo.

Una parte essenziale degli LWR è un generatore di vapore, che trasferisce la potenza dal circuito primario (collegato al reattore) al circuito secondario (collegato alle turbine). Analizzando le prestazioni di uno scambiatore di calore a piastre compatto (PHE) impiegato come generatore di vapore all'interno del sistema di rimozione del calore di un SMR nell'ambito del progetto ELSMOR, la seguente tesi tenterà di colmare una lacuna in questo campo. La comprensione di tale componente aiuterà l'ulteriore sviluppo e la proliferazione degli SMR.

Dopo una breve panoramica sugli SMR e sulla struttura dell'impianto di ELSMOR, viene eseguita un'analisi dello scambiatore di calore a piastre compatto funzionante con fluidi liquido-liquido e liquido-evaporante. Le correlazioni di scambio termico più diffuse in letteratura sono presentate e validate sui dati sperimentali raccolti durante la campagna di test SIET e quindi confrontate con il coefficiente di scambio termico estratto dai dati grezzi. Successivamente viene creata una correlazione di trasferimento di calore ad hoc per ottenere una migliore corrispondenza con i risultati sperimentali.

Parole chiave: coefficiente di scambio termico, scambiatore di calore a piastre compatto, SMR, ELSMOR

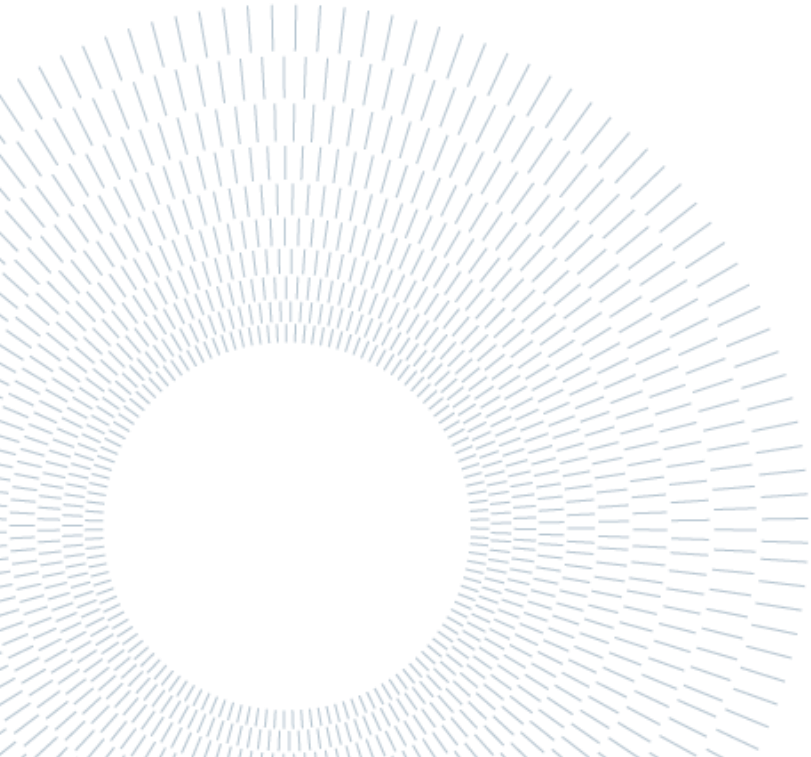

Contents

Introduction

The worldwide push to decarbonize the energy industry and slow down climate change must include nuclear energy. Although renewable energy sources like wind and solar are expanding quickly, they are still unable to offer the baseload electricity that fossil fuels and nuclear energy have historically offered. Moreover, the intermittency of renewable sources necessitates alternative energy sources, and nuclear energy offers zero-emission energy when coupled with improved waste management and security measures. Also, compared to solar or wind farms, nuclear power facilities require far less land, which could be important, especially in nations where population density and land access are challenges. Combining nuclear energy with renewables and energy efficiency can aid in the shift to a low-carbon economy and provide benefits for the economy, the environment, and national security. As a result, stakeholders and policymakers should be aware of nuclear energy's potential to reduce carbon emissions while ensuring energy security and reliability.

Small modular reactors (SMRs), which are more cost-effective than conventional large-scale nuclear reactors due to their smaller size and more straightforward design, also have better safety and security features. SMRs are receiving a lot of attention and investment due to the increasing demand for clean, dependable, and inexpensive energy worldwide. If they are successfully deployed, they might have a big impact on the future of nuclear power and our move toward a carbon-free energy system.

Just scaling of LR major components like pumps, steam generators, pressurizers, etc. is insufficient. Current and emerging technologies need to be thoroughly studied and tested. An essential part of LWRs is a steam generator, which transfers power from the primary loop (attached to the reactor) to the secondary loop (connected to the turbines).

By analysing the performance of a compact plate heat exchanger employed as a steam generator as part of the heat removal system of a SMR under the ELSMOR project, this thesis will attempt to close a gap in that effort.

The HVAC&R (heating, ventilation, air-conditioning, and refrigeration) industry frequently uses plate heat exchangers, for instance in the food industry. They have never before worked in the nuclear industry, precisely for the previously stated goal.

Understanding such component will help the further development and proliferation of SMRs.

1 SMR overview

In this first chapter, a brief overview of the nuclear energy sector will be discussed, followed by an in depth analysis of both technical and economical SMR's features.

1.1. EU nuclear energy context

The nuclear industry in Europe is a complex sector that plays a significant role in the region's energy mix. There are currently 103 nuclear reactors in operation in 13 EU member states, which generate approximately 25% of the region's electricity, around 50% of EU low-carbon electricity generation and support around 1 million jobs (Figure 1Figure 1). These reactors are located in a number of different countries, including France, Germany, Sweden, Ukraine, and the United Kingdom. [1] [2]

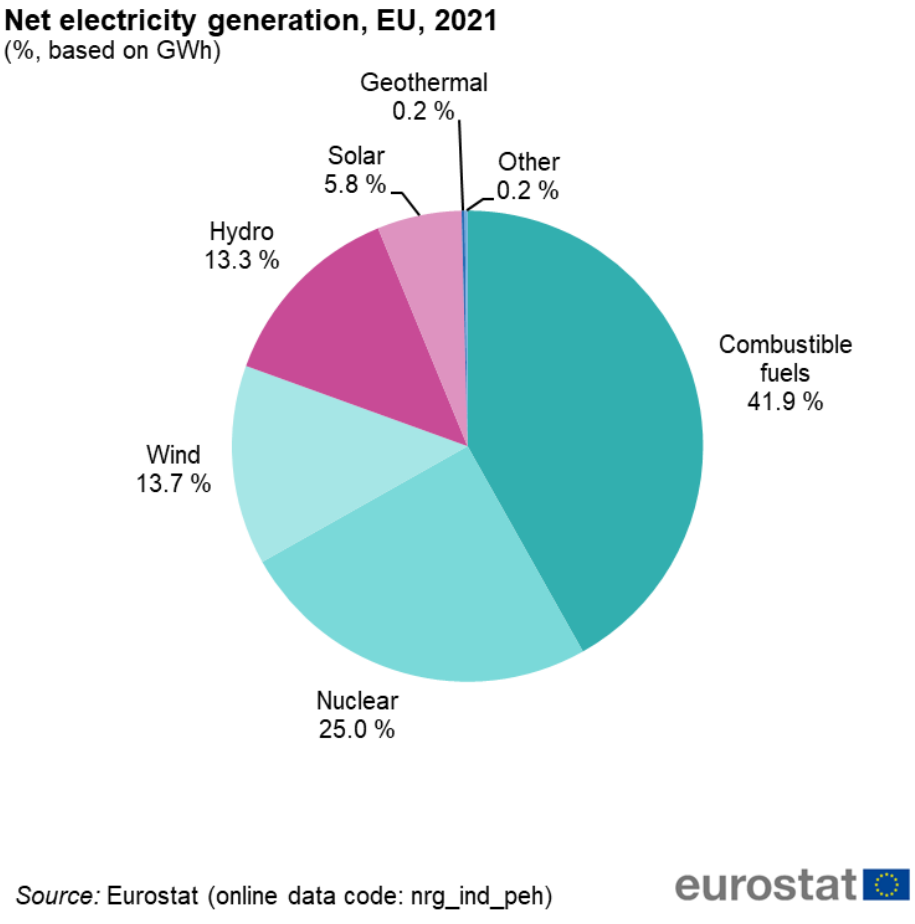

Figure 1: Net electricity generation EU 2021.

To achieve its ambitious goals for clean energy technology deployment, including nuclear energy, the European Union (EU) has been supporting the development of new nuclear technologies like small modular reactors (SMRs), which are an essential source of low-carbon electricity in the future.

However, the nuclear industry in Europe has also faced significant challenges in recent years. Many countries, including Germany and Switzerland, have decided to phase out nuclear energy as part of their efforts to transition to a low-carbon economy. In addition, the high costs associated with building and decommissioning nuclear power plants, as well as concerns about safety and waste disposal, have led to opposition to nuclear energy in some parts of Europe.

Despite these challenges, the nuclear industry in Europe remains an important source of electricity and is likely to continue to play a significant role in the region's energy mix in the coming years.

As previously mentioned, the EU has set challenging targets for the decarbonisation of its energy sector as part of its efforts to address climate change and reduce greenhouse gas emissions. The EU has committed to reducing its greenhouse gas emissions by at least 55% by 2030 compared to 1990 levels (fit 55 package) and is working to achieve carbon neutrality by 2050. To achieve these goals, the EU is promoting the development of renewable energy sources, such as solar and wind power, and is also supporting the deployment of advanced nuclear technologies including SMRs. [2]

In addition to these efforts, the EU is also working to improve the safety and security of its nuclear energy sector through initiatives such as the European Nuclear Safety Regulators Group (ENSREG) and the Nuclear Safety Directive. These efforts are aimed at ensuring that nuclear energy is produced safely and sustainably in Europe.

1.2. Small Modular Reactors

Small modular reactors (SMRs) are a type of advanced nuclear technology that have the potential to play a role in meeting Europe's energy needs. SMRs are smaller, simpler, and more flexible than traditional nuclear reactors, and they can be used to generate electricity, heat, or hydrogen.

They are generally defined as nuclear reactors with power outputs between 10 megawatts electric (MWe) and 300 MWe. SMRs present several technical features that enhance construction predictability and lead to potential reductions in construction costs and delivery times, because by design they incorporate higher levels of modularization, standardization, and factory building. Moreover, they adopt inherent safety features and take advantage of the “series effect”. [3]

Even though recently there has been a spike in interest around SMRs, they are actually not such a revolutionary technology as it is presented to us. Indeed, small size nuclear

reactors were first developed in the 60's during the cold war as naval and submarine propulsion systems.

These SMR designs use a variety of coolants and fuel forms, for example, and have different technology readiness levels (TRLs) and licensing readiness levels (LRLs). Most of them can be grouped into the following five categories [3]:

- Single Unit LWR-SMRs
- Multi module LWR-SMRs
- Mobile/Transportable SMRs
- Generation IV (Gen IV) SMRs
- Micro modular reactors (MMRs) – less than 10 MWe of capacity

In general, the LWR-based SMR concepts are the most mature with the highest TRLs and LRLs, and they are expected to be the earliest ready for commercial deployment. Several ideas are being developed or are already in use commercially, such as CAREM in Argentina and ACPR50S in China. By 2030, initial prototypes of other designs that are making substantial licensing progress could be built. These technologies, which draw on decades of operational and regulatory experience, are scaled-down evolutions of the Gen II and Gen III/III+ reactors currently in operation around the globe.

In contrast to LWRs, Gen IV technologies use alternative coolants, such as liquid metal, molten salt, or gas, and various system layouts. Although Gen IV-based designs don't have the same operating and regulatory experience as LWRs do, and some areas still require more research, they still gain from a long history of prior research and development that developers and regulators can draw from. Metal-cooled and gas-cooled systems, some of which are presently in use or being built, are the most developed Gen IV designs. Due to their higher outlet temperatures (see Figure 1) and advanced nuclear fuel cycles, these designs might also offer unique chances to think about non-electric uses.

According to the International Atomic Energy Agency (IAEA), approximately 72 SMR concepts are currently under development, which represents a 40% increase from 2018 [4].

1.2.1. Key design advantages

A few important SMRs characteristics have already been briefly discussed. It is only appropriate a thorough examination of the following features:

- Integral Designs: All the components of the nuclear steam supply system (NSSS) are fitted inside a single vessel. This allows for a simpler configuration, operation, and maintenance and enhanced safety.
- Inherent safety: A higher reliance on passive cooling systems allows for more simplified designs and streamlined operation and maintenance. Moreover, the

higher surface-to-volume ratio allows for heat removal systems previously not considered, such as natural air circulation. The inherent safety is also assured by the integral and simplified design, since the occurrence of typical accidents (LOCA or leakage points) is less probable. Lastly, innovative design choices like control rod drive mechanism (CRDM) avoid rod-ejection accidents.

- Lower core inventories: Workers receive lower radiation exposure levels because less shielding is needed on-site. Emergency planning zones may not be as necessary off-site because of the smaller inventory. These advantages, in addition to inherent passive safety systems, might allow for the placement of some SMRs nearer to areas where energy is required or where normally large reactors couldn't' be placed.
- Improved modularization and manufacturability: How readily the different components can be manufactured, transported, lifted, and installed is directly influenced by their weight and size. SMR designs' smaller size makes it possible to implement more ambitious modularization plans and new manufacturing methods. This topic will be further discussed later.
- Enhanced flexibility: SMRs could accomplish improved load following modes due to inherent design features and through the optimization of multi-module unit operation by utilizing the manoeuvrability capabilities of current. More broadly, SMRs' flexibility includes their deployment skills (such as less restrictive siting requirements) and variety of products. (combined heat and electricity production).

1.2.2. Key economic advantages

Historically, reactor designers have scaled up reactors to bigger sizes in order to benefit from economies of scale. The business case for SMRs is supported by economies of series production, which depend on four key cost drivers: design simplification, standardization, and modularization, while maximizing factory fabrication and minimizing on-site construction. This helps to balance out diseconomies of scale and increase competitiveness. The advantages of serial construction have been extensively studied in other fields, such as shipbuilding and airplane manufacturing, where serial production has led to learning rates of between 10% and 20%. Serial manufacturing may also result in the amortization of non-recurring expenses like costs associated with design certification and research and development for the initial SMR units.

The market for a single design must be sufficiently large in order to achieve serial factory fabrication. It is expected that cooperation among nuclear safety regulators to increase the harmonisation of licensing systems will be crucial in facilitating the development of this global market. The summary of the economic factors influencing SMR competitiveness is shown below. (Figure 2)

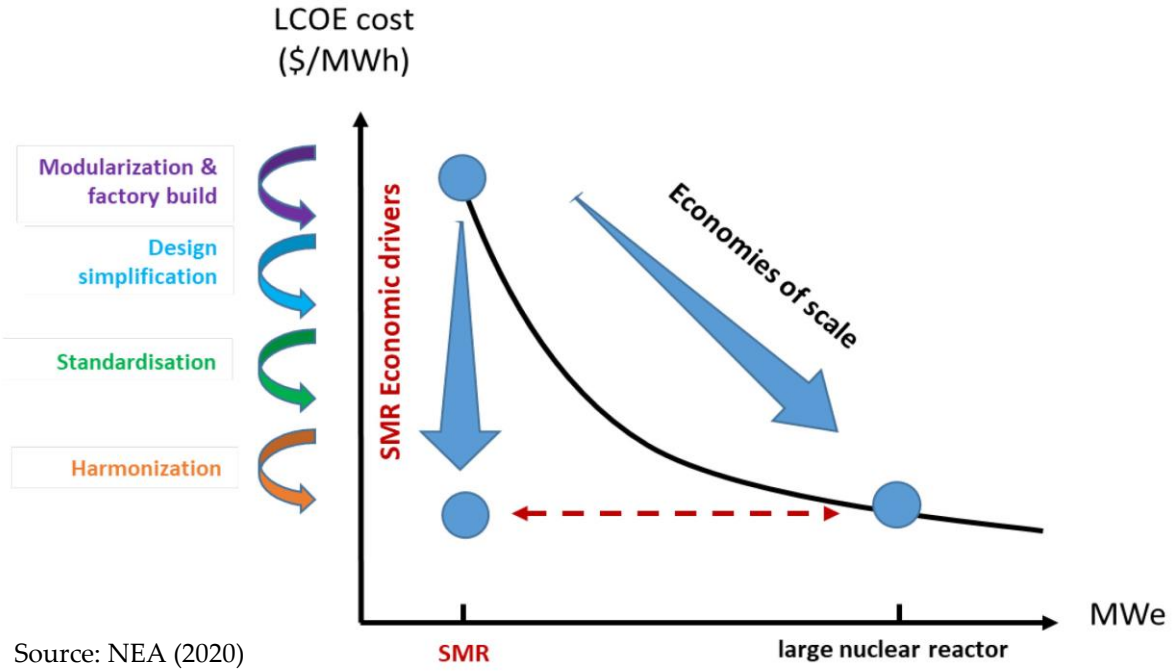

Source: NEA (2020)

Figure 2: SMR key economic drivers to compensate for diseconomies of scale.

Modularization and factory based construction

Construction can be made more straightforward by breaking the plant up into packages (modules) that can be manufactured in a facility, transported, and then put together on site. The building and/or pre-assembly of modules away from the construction site in a dedicated factory, where labour productivity and quality control can be expected to be higher and project management risks can be reduced, is one way in which cost savings can be achieved. Furthermore, a component size influences greatly its transportability, therefore some SMRs design allow transport of its modules using conventional trucks, ships, or rails. The advantages of modular building have been proven in other sectors, including shipbuilding and airplane manufacturing, where the factory-based modularization of construction has reduced costs. Modularization and factory fabrication are already used for about 30% of the building of nuclear reactors, and their application could rise to 60% to 80% with the adoption of more ambitious strategies made possible by the smaller size of the components. The repeatability of tasks could lead also to increased labour efficiency. Moreover, the cost of sophisticated manufacturing techniques (such as additive manufacturing or welding) that would otherwise be challenging to implement on-site can be done, can be cut down. Finally, the shorter and more predictable construction durations that would come from modular construction would eventually lower the risk premiums anticipated by some investors. Additionally, it would mean a shorter time to market, which might improve the prospects for the SMR market.

Modular building may still have some disadvantages. Firstly, additional up-front engineering work is needed to recognize and properly design the various modules;

secondly it is also necessary to purchase the materials and components for the various modules, which raises the upfront investment requirements.

In general, the key challenges for SMRs regard mainly problems due to licensing, since (at least in Europe) there is limited experience of safety authorities and due to the risk associated with building a first of a kind (FOAK) SMR.

Design simplification

The integral configuration of SMRs requires less materials and active components, such as reactors cooling pumps and their associated auxiliary systems, compared to a large reactor. Some SMRs are designed to operate with natural circulation. Moreover, SMRs require simpler safety systems, with less redundant and auxiliary components. Additional simplification opportunities are at the level of the overall plant design, including the use of commercial, off-the-shelf components (COTS) and by creating common plant infrastructure, such as shared turbine buildings and control rooms. These various simplification techniques might result in lower building costs for SMRs, either directly by reducing the quantity and size of parts and systems or indirectly by improving project management. For instance, design simplification might lower the risks of rework and decrease building delays, both of which have recently affected Gen III+ first-of-a-kind projects. Prime example of large reactors projects whose poor management led to delays and extra cost are Olkiluoto 3 and Flamanville 3 power units.

Standardisation

Higher degrees of standardization are offered by SMR designs. Large reactors have demonstrated to benefit from the standardization of design and subsequent replication because it encourages learning-by-doing and helps to mobilize the supply chain through lengthy new build programs. The standardization of reactor architectures could be aided by additional characteristics, such as maximizing the use of COTS components in SMR designs. Early involvement of the nuclear supply chain will play a crucial role in supporting the design standardization process as SMRs progress to the demonstration and deployment stages.

Scalability

One of the main advantages of SMRs is their scalability. They can be built in smaller increments, allowing for a more flexible and phased approach to nuclear power generation. Moreover, the possibility to add modules further on and start generating electricity helps reduce upfront costs and allows investors to be able to respond to changes in energy demand and in financing, which could improve the management of financial risks.

Flexibility & decarbonisation

SMRs can operate flexibly in electricity networks with variable residual loads, such as in areas pursuing the high penetration of variable renewable energies (VREs), due to their inherent load-following characteristics (wind, solar photovoltaic [PV]). Support for VRE implementation could also be seen from the perspective of integrated "hybrid" energy systems, which combines SMRs with non-electric applications (hydrogen, synthetic fuels, district heating and desalination) to aid in the integration of wind and solar PV. These integrated systems are a desirable choice economically because they can increase the energy system's overall reliability and resilience. Additionally, SMRs could aid in the decarbonisation of other energy industries. For instance, district heating applications, which can readily be met by LWR-SMRs, require output temperatures between 80 and 200 °C. For instance, using SMRs for district heating has recently been suggested as a practical way to site SMRs closer to demand and completely decarbonize the heat industry in Finland. Over the past few years, Saudi Arabia has also reported that it is interested in SMRs to satisfy its desalination needs. The King Abdullah City for Atomic and Renewable Energy (KA-CARE) and the Korea Atomic Energy Research Institute (KAERI) signed a memorandum of understanding in March 2015 to discuss the possibility of constructing two SMART reactors in Saudi Arabia.

SMRs are well-suited for countries with smaller energy markets or for communities that may not have the resources for a large nuclear reactor or may not have a fully developed grid. Another benefit is that they have a smaller footprint compared to large reactors, which means they can be more easily integrated into existing energy systems. SMRs also have the potential to be deployed in a variety of locations, including remote or off-grid areas where other forms of power generation may be challenging or expensive (e.g. KLT-40S in Russia).

1.2.3. Future estimates

The NEA investigated the potential market for SMRs in the near future (2035) and created two scenarios that represented market development uncertainty: a high deployment scenario that was optimistic and presupposed successful SMR licensing, factory production, and the creation of the supply chain that would enable cost competitiveness; A cautious low-deployment scenario, where a small number of projects, such as prototypes and plants in isolated locations, would be finished because SMRs are costly to construct and run (Figure 3). The former predicts up to 21 GWe of SMRs would be installed by 2035, which accounts for about 3% of the total installed world nuclear capacity and therefore SMRs would represent 9% of the total nuclear build in 2030-2035.

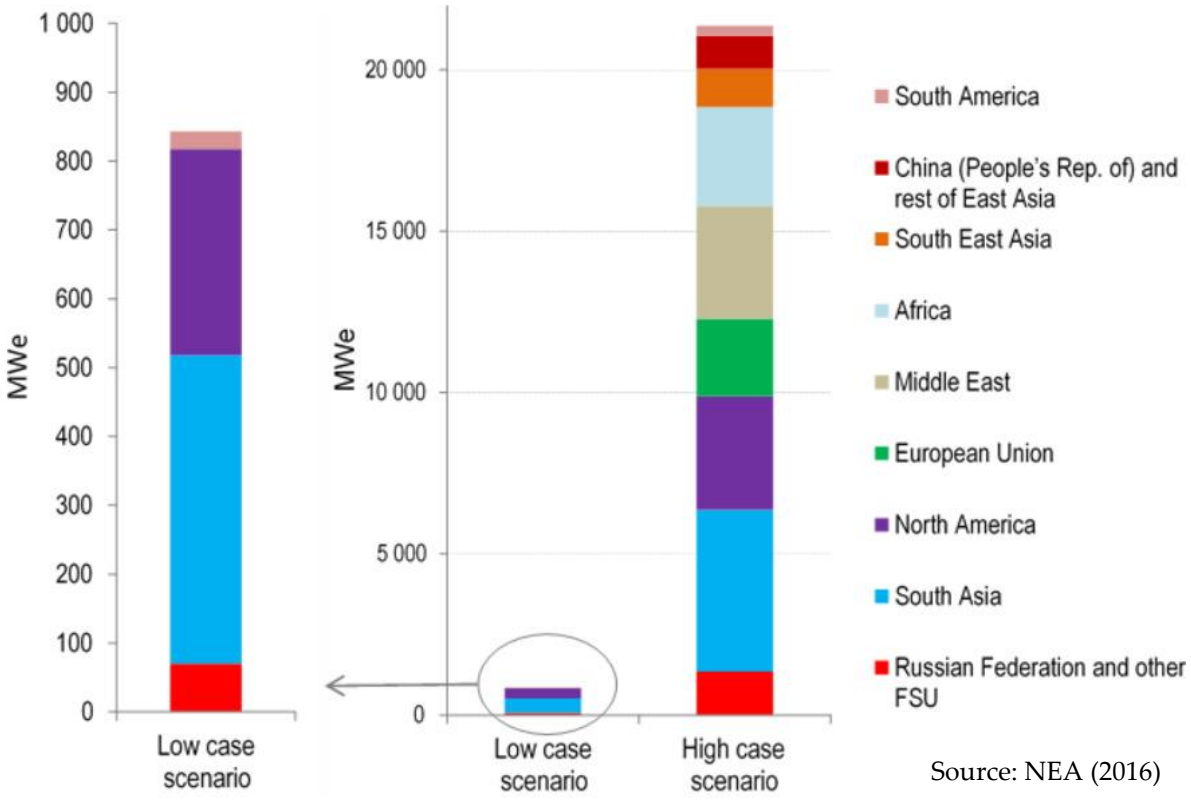

Source: NEA (2016)

Figure 3: Estimated SMR capacity by region in 2035

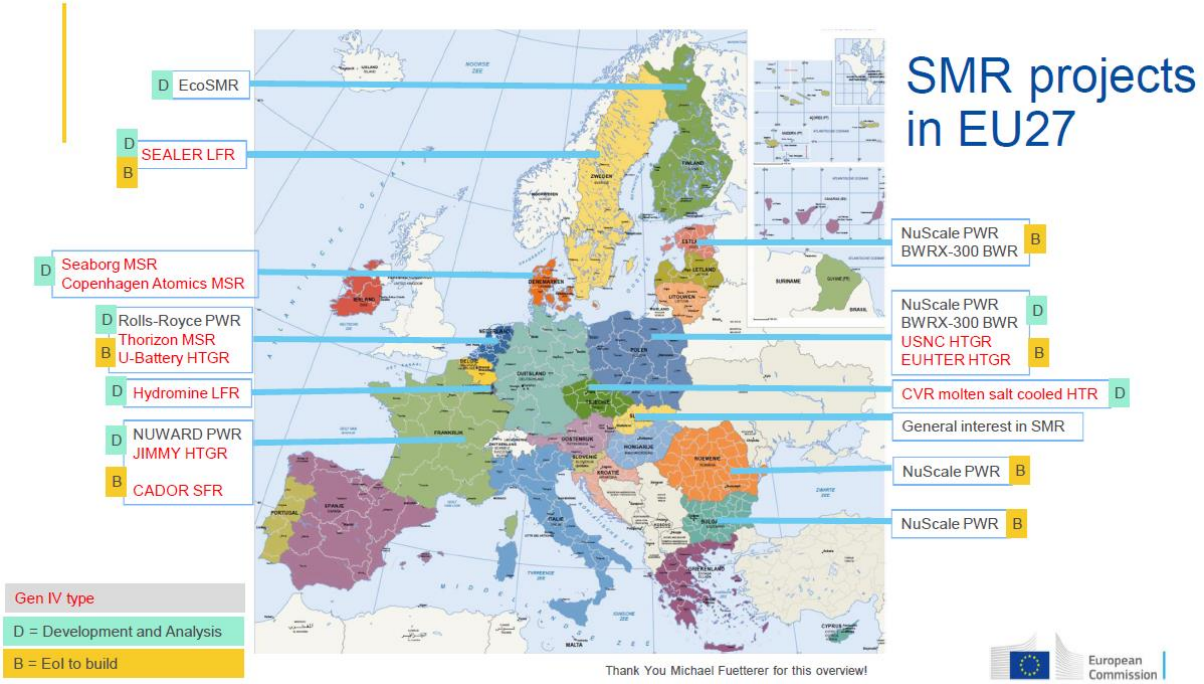

Figure 4: SMR projects in EU27

2 ELSMOR & SIET

The ELSMOR project is hereby presented, followed by a summary of SIET's facility main components and operational conditions. After a brief general explanations of plate heat exchangers, SIET's experimental campaign and main test results are displayed.

2.1. ELSMOR project

Internationally, the development of Light Water Small Modular Reactors (LW-SMRs) has reached a stage where numerous designs are being suggested for construction everywhere. In order to be able to react to this change, European stakeholders—including the business, regulators, support groups, and academia—must be ready. The ELSMOR (towards European Licensing of Small MOdular Reactors) project seeks to improve Europe's capacity to evaluate and create novel SMR concepts and their safety features. The work aims to both comprehensively examine the safety of LW-SMRs and to delve deeply into a set of issues that the consortium has determined to be the most important in ensuring that future SMRs comply with the safety goals set forth in the amended Directive 2009/71/Euratom.

ELSMOR improves light water SMR understanding and technology solutions on numerous fronts:

- Information collection, analysis, and distribution to diverse stakeholders, including the public, decision makers, and regulators, on the promise and challenges of Small Modular Reactors.
- Creation of high-level methodologies for assessing the safety of LW-SMRs.
- Enhancement of European experimental research infrastructure to aid in the assessment of unique safety aspects of future LW-SMRs.
- Improving European nuclear safety analysis codes in order to demonstrate the ability to analyse the safety of future LW-SMRs.

A cutting-edge analysis of the planned near-term LW-SMRs and their proposed safety features will be produced by the project. Based on experience with both big reactor analysis methodology and the implementation of such methodology for Generation IV reactors, a methodology for safety analysis for the novel LW-SMRs will be created. Analytical and experimental evaluations of the most important safety features will be used in the work on the passive safety systems of LW-SMRs in ELSMOR. The precise methods vary between the LW-SMR concepts, but in general, it's crucial to check that the passive safety functions are working and to validate the analysis codes. To show

how the developed safety case methodologies and models can be used in actual situations, they will be applied to a selected reference design. While concentrating on the safety aspects of the overall design, a particular emphasis will be placed on the safety features that are unique to large PWRs. [5]

The ELSMOR project is based on the experience of a consortium made up of technical support organizations, technical research centers, industrial partners, and universities that have a wealth of knowledge in European nuclear safety analysis and the creation and application of cutting-edge nuclear technologies.

- Finland: VTT, Fortum;
- France: EdF, TechnicAtome, Framatome, IRSN, CEA;
- Germany: GRS;
- Ukraine: Energorisk;
- EU: JRC-Petten;
- Italy: CIRTEN-POLIMI, SIET, ENEA;
- Lithuania: LEI;
- Switzerland: PSI;

Coordinated by the VTT Technical Research Centre of Finland, the project lasted from 09/2019 till 03/2023, for a total duration of 3,5 years. SIET s.p.a. (Società Informazioni Esperienze Termoidrauliche) is one of them. This small company based in Piacenza, Italy, is leader in the tests for the research and development of innovative components and systems for power production of nuclear origin.

ELSMOR has been split up into a number of parallel work packages. [6]

Identification of improved safety features of LW-SMRs, led by GRS

WP1 focuses on the identification of advanced or innovative safety features of LW-SMRs that potentially pose challenges to established safety demonstration approaches.

- Review of the European nuclear safety directive(s) and good practices on the safety assessment of LWR reactors,
- Screening of current LW-SMR designs (based on available material) related to improved or innovative safety features
- Summary of safety challenges for further consideration in the project

Development of safety analysis methodology for LW-SMRs, led by Framatome

WP2 focuses on developing a methodology with qualitative and quantitative recommendations to support the safety demonstration of LW-SMRs.

- Complementary methodology development
    - Assessing the applicability of technology neutral Integrated Safety Assessment Method (ISAM) developed by GenIV International Forum
    - Systems engineering approach
- Various aspects of SMRs

  - High-level objectives (reactivity control, core cooling, containment)
  - Multi-unit plants, human factors, decommissioning, fuel management

Core cooling safety functions, led by ENEA

Work Package 3 focuses on core cooling safety functions of integral LW-SMRs.

- Work to be performed is associated with safety analysis, development and assessment of codes and models
- Experimental investigations at SIET facility
  - Heat exchanger mock-up from TechnicAtome
  - Blind and post-test modelling, model development

Improved Safety Analysis Methods and Tools for Containment Safety Functions, led by GRS

The objective of this WP is the development, assessment, and validation of analysis methods and tools for the safety demonstration of improved or innovative containment safety function features of integral LW-SMRs in general and the currently proposed French F-SMR design as a reference SMR in particular.

Example of application of safety case methodology, led by EDF

An application of the developed safety case methodologies and models with a chosen reference design will be performed in order to demonstrate their applicability for real cases. The approach will focus on the safety features of the global design, but with special attention and effort on safety systems that differ from large PWRs.

- the application of the high-level methodologies developed in the Work Package 2 to the F-SMR,
- the working of the safety functions in an accident scenario, and
- the working of the safety functions in a severe accident scenario.

Synthesis, Recommendations and Dissemination, led by Fortum

WP6 focuses on stakeholder interaction and dissemination results of the project to recommendations to stakeholders. This will be performed throughout the lifecycle of the project.

- Identifying important stakeholders and analysis of their needs
  - Different dissemination strategies towards different stakeholders
  - Industry, general public, academia, decision makers
- Development of recommendations to stakeholders and future R&D work based on project outcomes
  - The organisation of an International Workshop
  - Dissemination of the project results

Education & Training, led by Cirten

WP7 targets the Education & Training of students and young researchers.

- Involvement of MSc and PhD students and young researchers in the ELSMOR R&D activities, the preparation and implementation of an International Summer School
- Design and broadcasting of Open Educational Resources (e.g. MOOC-like videos) on SMR concepts and ELSMOR findings

Regarding WP3, the need of an experimental facility in the ELSMOR project had basically three goals:

- Indicate the route on how to perform an experimental campaign to the European Regulator called to certify SMRs in Europe;
- Test a passive decay heat removal system, to be potentially installed on the E-SMR, based on a compact plate-type heat exchanger included in a natural circulation loop that rejects heat into a water pool;
- Validate different codes in pre-test and post-test analyses;
- For the future: to investigate open items like heat exchanger fouling factors, instabilities at low natural circulation flowrates, etc.

2.2. ESLMOR facility at SIET

The facility simulates the Emergency Heat Removal System (EHRS) of the E-SMR with an approximate power/volume scaling factor of 1:50 and 1:1 factor in elevation. It consists of a natural circulation loop that, coupled to the primary side by a type-plate heat exchanger (S-CSG Safety-Compact Steam Generator), rejects the decay heat to a water pool by means of a vertical tube heat exchanger. The use of a plate heat exchanger (PHE) in an integral type SMR has the potential advantage of high-power transfer in an extremely compact configuration. It is the first time this kind of heat exchanger is proposed to be part of a nuclear power plant for civil use. Figure 5 shows a simplified scheme of the ELSMOR facility at SIET.

The primary loop is equipped with a pump and an electrical heater suitable to supply water to the primary side of the S-CSG. Working under forced circulation, it can be operated either with a single-phase liquid or in two-phase conditions with the primary side in saturation. The separation occurs at the S-CSG bypass/steam-water separator, a vertical 10-inch tube. A flow restrictor is inserted suitable to provide the necessary pressure drops to the circuit and split the mass flow supplied by the pump part into the CSG and part into the by-pass. The separator size is suitable to allow a steam/water separation by gravity, due to the relatively small velocity of steam, allowing two kinds of circulations: natural for steam to the CSG and forced for liquid to the pump. The fine control of the required mass flow is performed by means of the loop control valve. The CSG water inlet temperature is controlled by varying the electrical heater power. The secondary side operates in two-phase natural circulation driven by heat provided by the S-CSG (heated-up by the primary side) and rejected in a water pool (heat sink)

containing a submerged vertical tube heat exchanger. The S-CSG is a commercial brazed plate type heat exchanger by TEMPCO, Model TCBC2102.

Table 1: Reference E-SMR technical specifications

Reference E-SMR	
Electric power	≈ 170 MW
Thermal power	≈ 515 MW
Decay power per loop	≈ 30 MW
Decay power ≈ 10% reactor power/2 ≈ 26 MW	

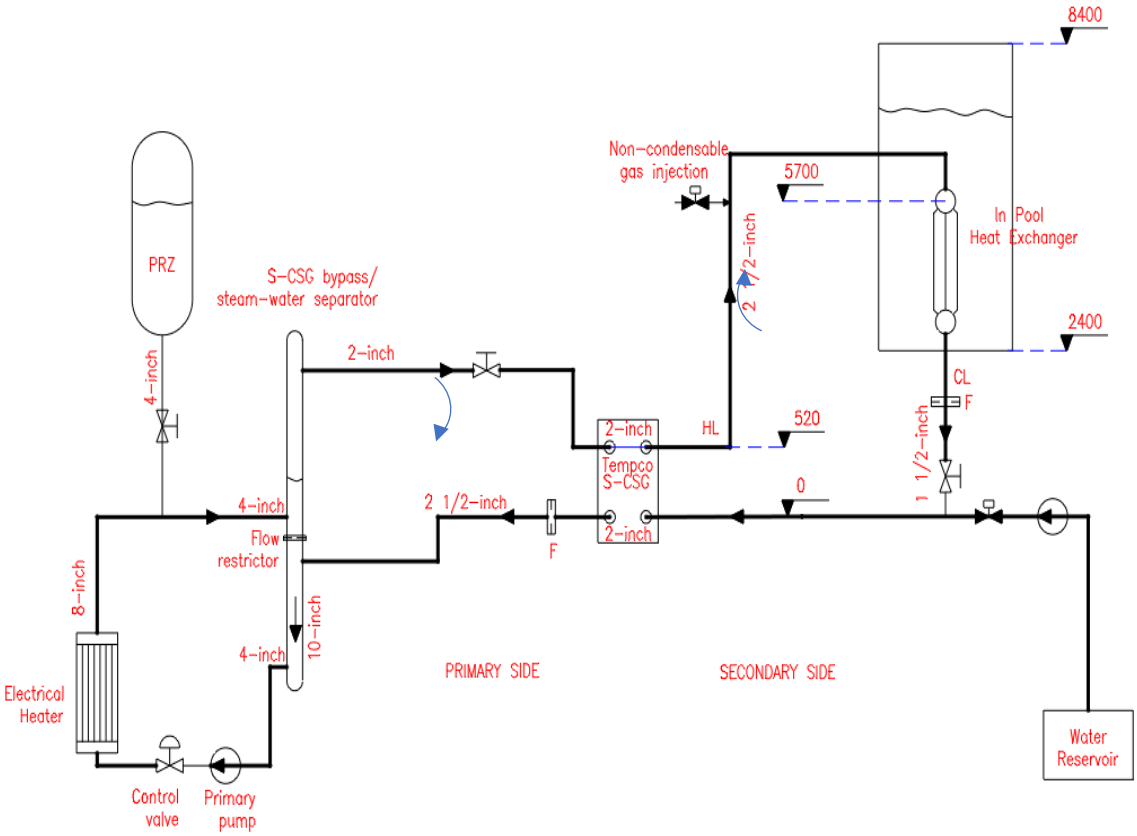

Figure 5: ELSMOR facility simplified scheme.

Table 2: ELSMOR facility technical specifications

ELSMOR		
Total height	≈ 15 m	
Power	≈ 1 MW	
Primary side design	P = 13 MPa	T = 330°C
Secondary side design	P = 10 MPa	T = 310 °C
In-pool HX	5 tubes, 2-inch diameter	≈ 2 m lenght
Cylindrical water pool (atmospheric pressure)	≈ 5 m^3 volume	≈ 6 m height

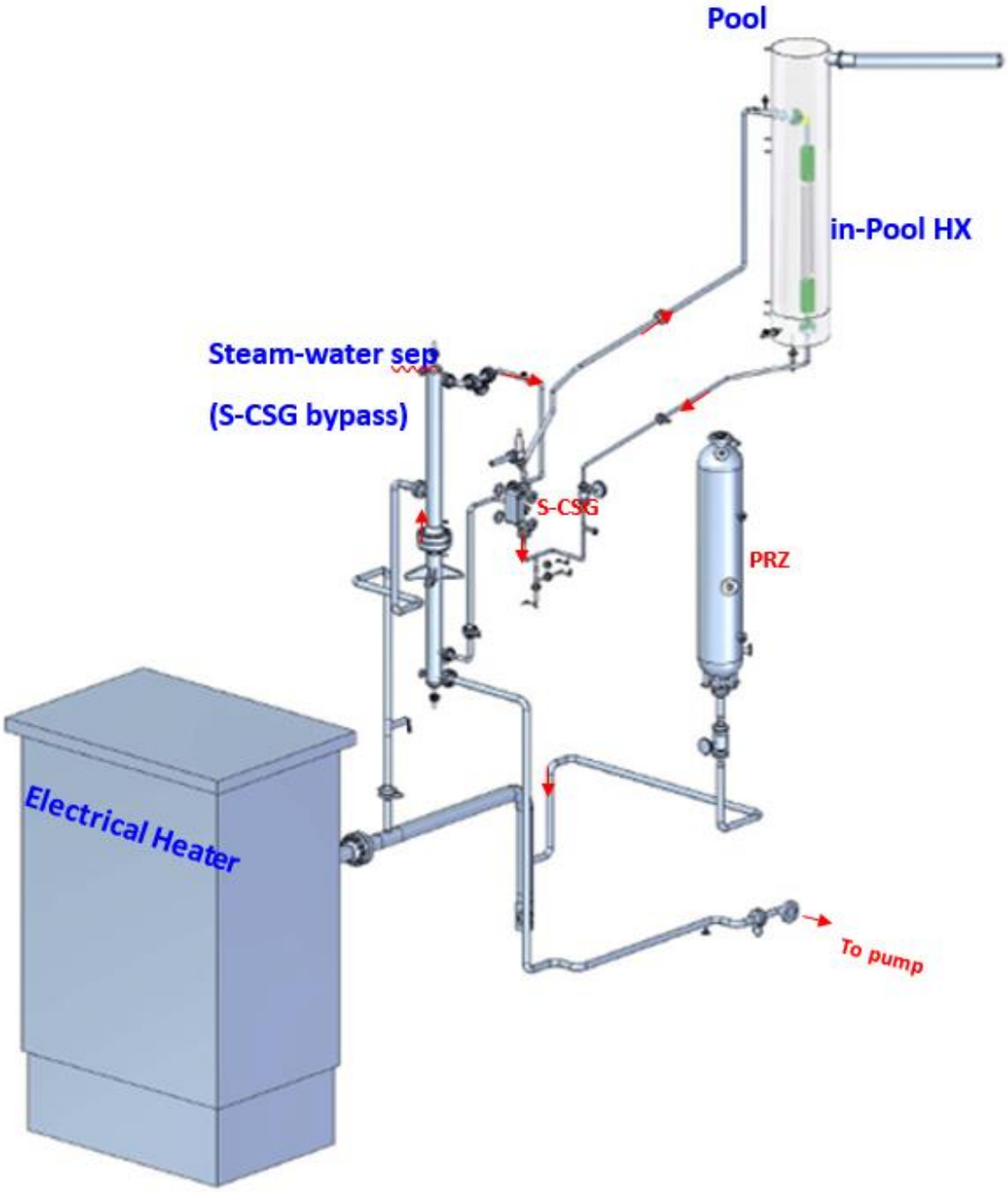

Figure 6: View of ELSMOR facility

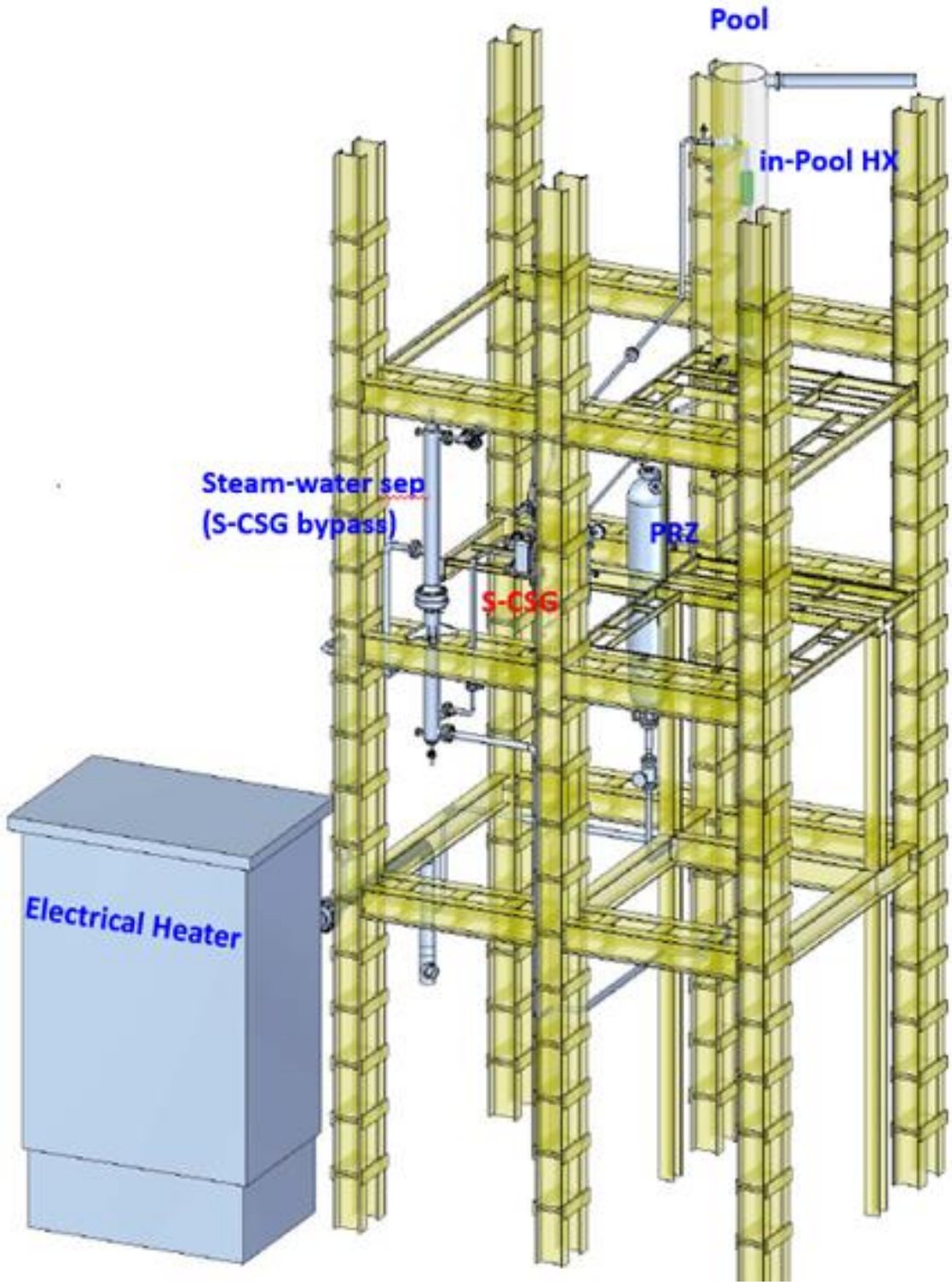

Figure 7: View of ELSMOR facility on the existing load-bearing structure

Figure 8: S-CSG before installation

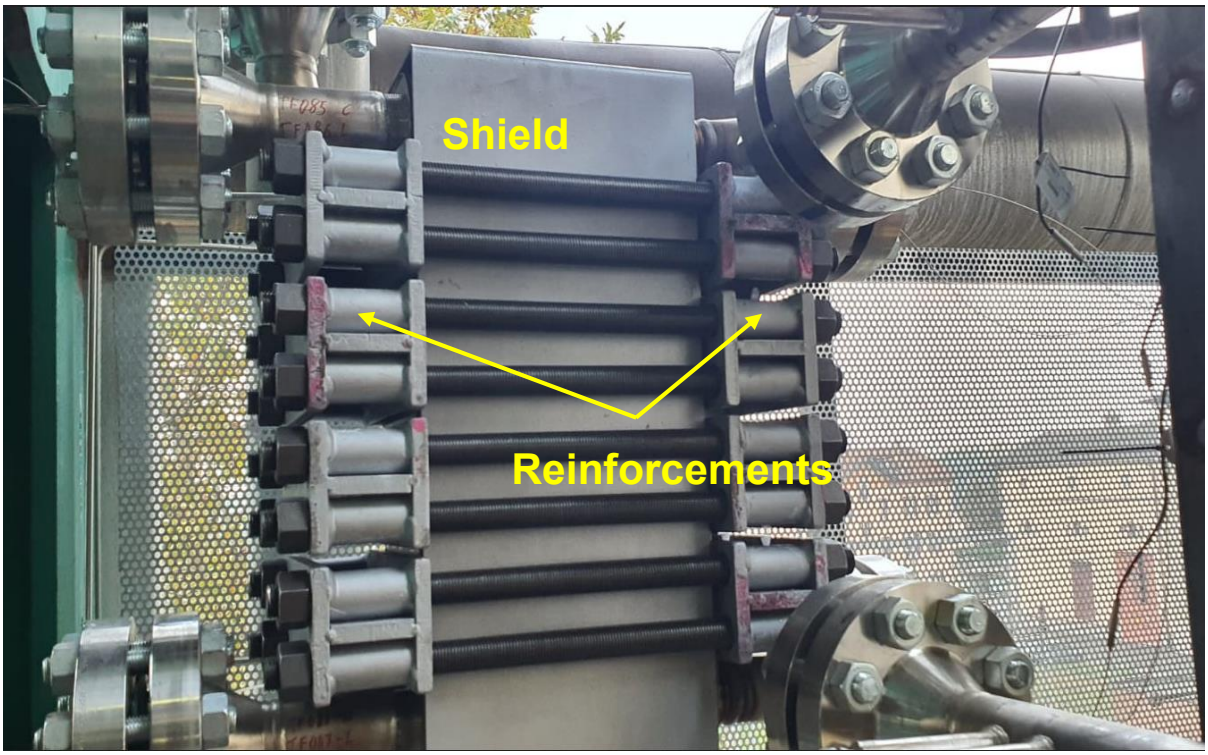

Figure 9: S-CSG after installation without thermal insulation. Reinforcements were added to ensure its structural integrity during operation.

Figure 10: S-CSG and primary side

Figure 11: HX - Pool container

Figure 12: Tube heat exchanger before installation inside the pool

2.2.1. Plate Heat Exchanger

A plate heat exchanger (PHE) is made up of several parallel plates that are stacked one on top of the other to create a network of channels that enable fluid to pass between them. The channel in which the fluid moves is created by the space between two adjacent plates. A plate is always in contact with the hot fluid on one side and the cold fluid on the other thanks to inlet and outlet holes at the corners of the plates that enable hot and cold fluids to pass through alternating channels in the exchanger (Figure 13). These plates are typically corrugated to enhance turbulence, the thermal exchange surface, and to give the exchanger mechanical rigidity. The plates are usually made of titanium, aluminium, and stainless steel (AISI 304, 316). The fluid is forced along a tortuous route by the plates' corrugation, leaving a pace (corrugation height b) of between 1 and 5 millimetres between adjacent plates. By creating configurations that are either counter-current or co-current, the fluids can cross the channels in parallel (most frequent option) or in series. When there is a low flow rate for each fluid but a high heat jump, the serial arrangement is used. The biggest issue is when there is a large pressure drop and an imperfect counter current. The most popular design is parallel with counter-current channels because it allows for high flow rates and moderate temperature drops. (Figure 14) [7]

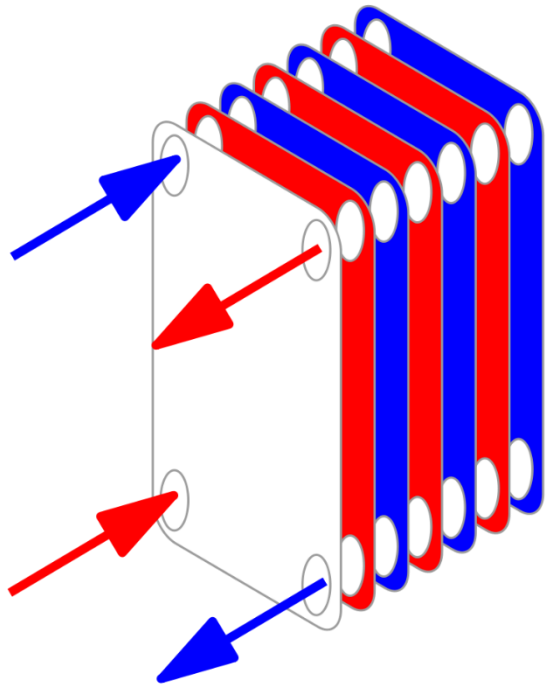

Figure 13: Simplified scheme of a PHE. (Source: Wikipedia)

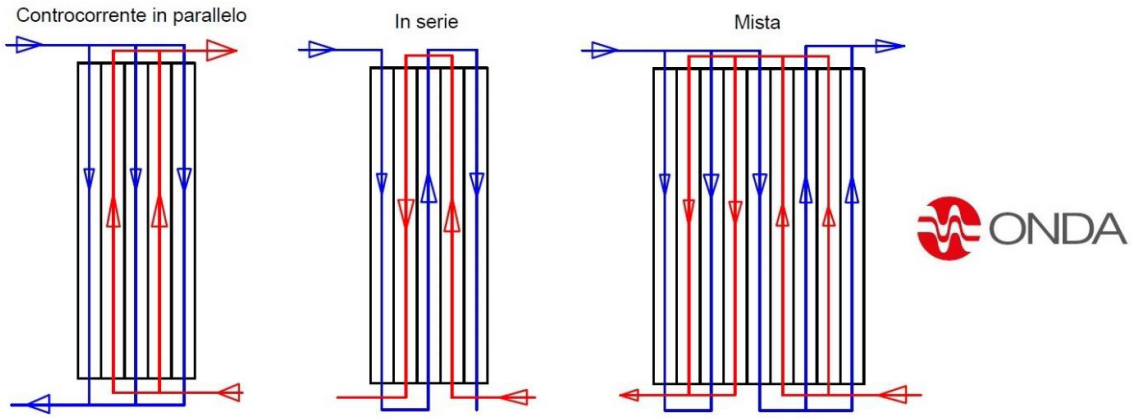

Figure 14: Different possible flow configurations. (Source: Onda S.p.A.)

An irregular supply of all channels simultaneously is one of the most frequent issues with plate heat exchangers. In order to balance the pressure decrease, the fluid actually has a tendency to distribute more evenly in the first channels than the last ones. The performance of the exchanger as a whole decrease as the number of plates rises due to a drop in even distribution. The two most common kinds of plate heat exchangers are: Heat exchangers with brazed plates (BPHE) and plates (PHE). (Figure 15)

Figure 15: Gasket PHE (left) and Brazed PHE (right). (Sorces: Onda S.p.A. and Wessel company)

Braze Plate Heat Exchangers

As a result of the plates being brazed in a furnace at 1100°C, brazed plate heat exchangers don't need headers, tie bars, or sealing seals. A sheet of brazing substance (typically copper, but also nickel) is sandwiched between the plates during assembly (Figure 16). The pack is then compressed and baked for a while. Compared to a gasket-based exchanger, the BPHE exchanger is smaller, lighter, and less bulky. The gaskets and the frame are both handled by the brazing material.

Figure 16: Cross section of a BPHE (Source: Onda S.p.A.)

In order to produce a lattice contact, these exchangers are typically used with chevron corrugated plates, which are assembled by alternately orienting the corrugation directions by 180° (Figure 17). Two coupled plates' corrugations cross at these places, forming a dense network of contact points that improves heat transfer and provides pressure tightness.

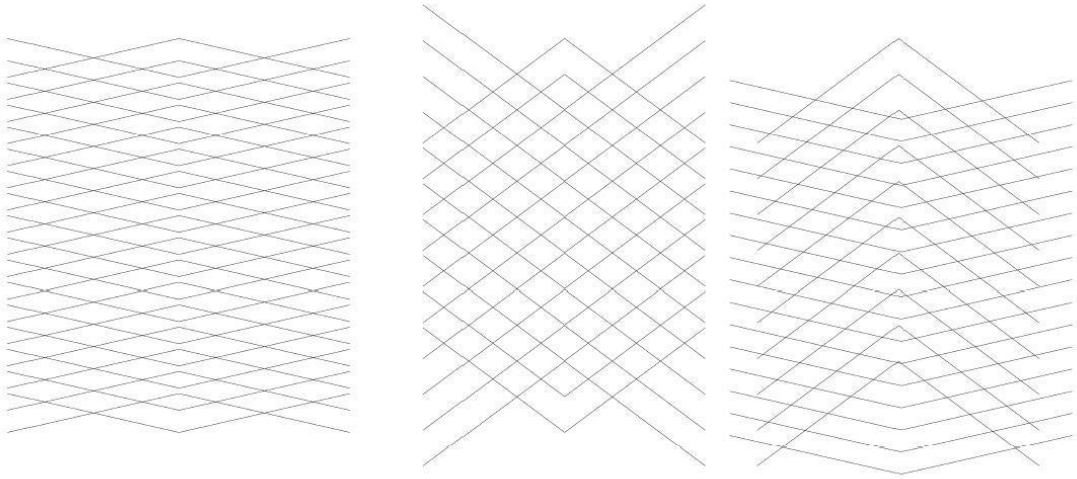

Figure 17: "Herringbone" pattern for different chevron angles (Source: Onda S.p.A.)

In this manner, the flow transitions from laminar to turbulent for low flow rates, and the fluid turbulence is high even at low nominal input velocities. Figure 18 depicts a cross section of an exchanger with 8 plates total (only 6 of which are contributing for heat exchange), and it can be seen that there are 4 channels for the hot fluid (in red) and 3 channels for cold flow fluid (in light blue).

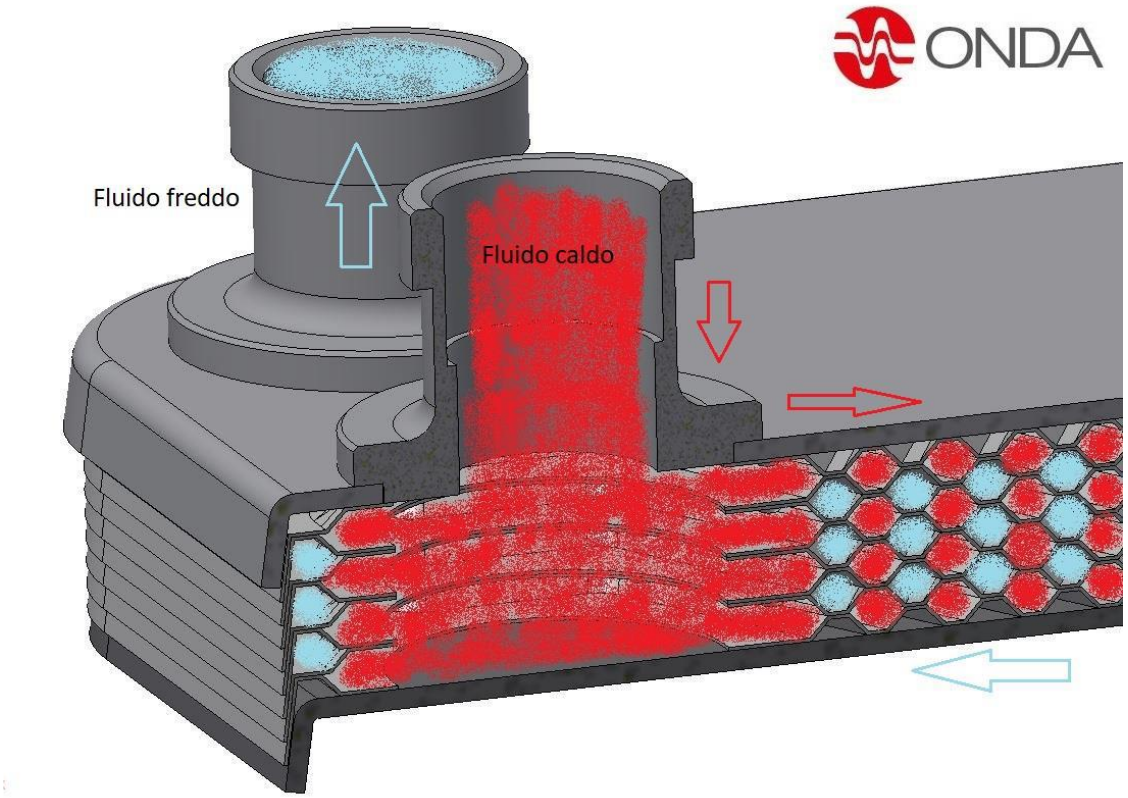

Figure 18: BPHE cross section with highlighted hot and cold flows (Source: Onda S.p.A.)

The primary drawback of these exchangers is that they cannot be removed, making maintenance and cleaning either impossible or very difficult. Additionally, there is no flexibility because the number of plates cannot be altered in any way.
The main plate parameters are shown in Figure 19:

- Corrugation height b;
- Corrugation pitch λ;
- Chevron angle β;
- Enlargement factor ϕ, defined as the ration between the actual heat transfer surface and the projected heat transfer surface;

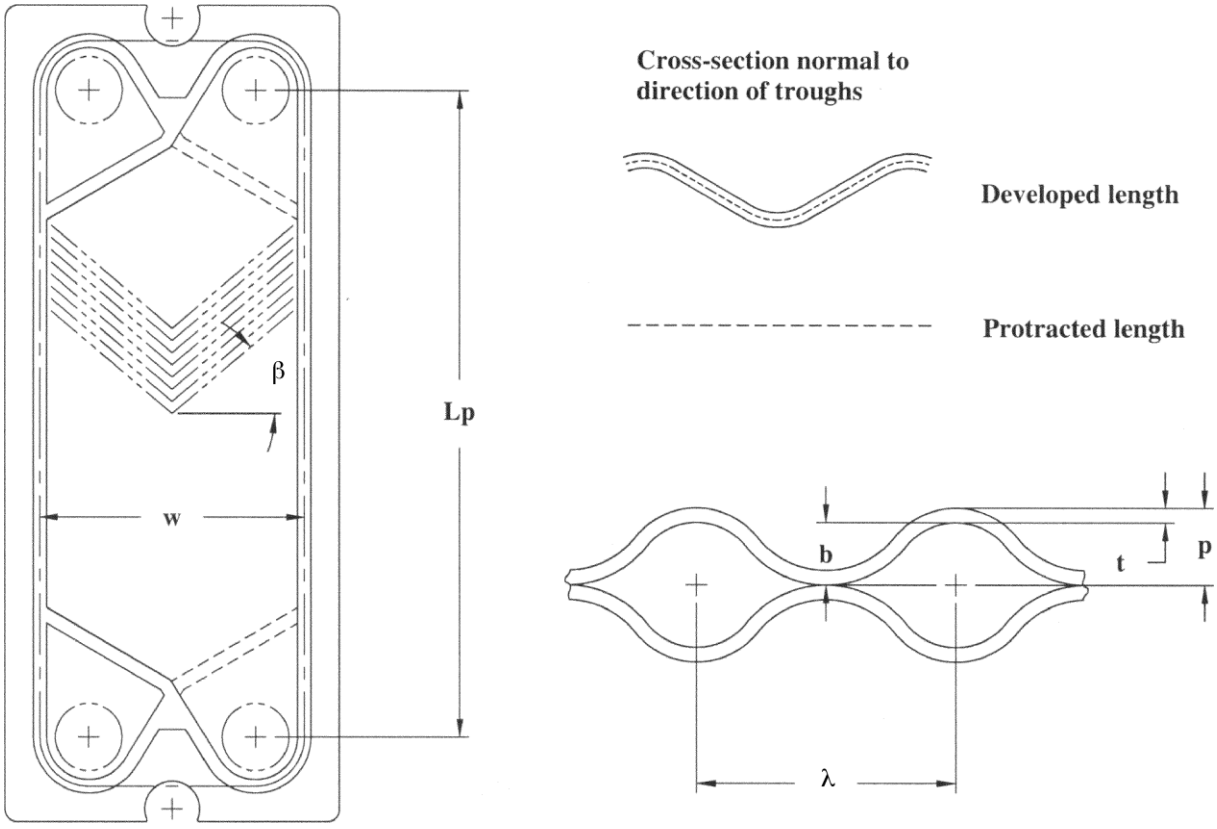

Figure 19: Plate parameters

Of them all, the chevron angle has the biggest influence on thermal exchange and on pressure losses. A smaller β angle (< 45°) creates less points of contact, inducing a lesser degree of turbulence therefore a lower heat exchange coefficient and lower pressure drop. Conversely, a high angle β (> 45°) is correlated with a higher heat transfer coefficient and higher pressure drops. Therefore, it is crucial to find a compromise angle between high exchange ratios and allowable load losses. The heat exchange coefficients are also impacted by the corrugation height b because a deeper layer produces more turbulence. Not only, but corrugation height b and pitch λ affect the plate surface, therefore influencing the enlargement factor ϕ. Finally, also the length L and the width W of the plate impacts, to a lesser degree respect to the previous parameters, the performance. In general, a high ratio between plate length and width gives high exchange rates but higher-pressure losses [8]. Lastly, some derived plate parameters worth mentioning are:

- $d_e = 2b$, equivalent diameter defined as twice the corrugation height b
- $d_h = \frac{d_e}{\Phi} = \frac{2b}{\Phi}$, hydraulic diameter defined as the ratio between the equivalent diameter and the enlargement factor ϕ
- $A = bW$, transversal cross section area

2.2.2. TEMPCO TCBC2120

Table 3: TEMPCO model TCBC2120 specifications

Design conditions		
	Primary side	**Secondary side**
Pressure (bar)	130	100
Temperature (°C)	330[1]	310[1]
Operating conditions		
	Primary side	**Secondary side**
Pressure (bar)	1-120	0.023-80
Temperature (°C)	20-320	20-T_ps
Mass flow rate (kg/s)	≈ 3.9	≈ 0.4
Pressure drops (kPa)	31.6 (at 3.9 kg/s)	14.4 (at 0.4 kg/s)

SIET acquired from TEMPCO the TCBC2120*130 model, an BPHE that works under parallel counter-current configuration and whose technical specifications are shown in Table 3. The "130" refers to the number of brazed plates composing such heat exchangers, of whom only 128 are active plates, since like in any other PHE, the 2 outmost plates don't contribute to the overall performance. Other relevant information are as follows:

- Primary and secondary side volumes ≈ 10 L each side (with 130 plates)
- Power ≈ 600 kW
- Height ≈ 0.5 m
- Width ≈ 0.2 m
- Thickness ≈ 0.30 m
- Single plate heat transfer surface = 0.095 m²
- Total heat transfer surface = 12.16 m² (0.095*128)
- Chevron angle $\beta = 45°$

Compared to Figure 8, initially this BPHE presented itself as in Figure 20 (A), that is to say without any of the 4 input/output nozzles for the fluid or any of the 4 supplementary input/output nozzles for the instrumentation installation. As mentioned previously, the HX was eventually equipped with a mechanical cage (made of plates and bolts) designed to withstand the maximum pressure in case of high temperatures and with a metallic shield on the access side.

[1] Certified (CE) design temperature of TEMPCO HX is 200°C for marketing needs. Manufacturer reported several cases of use outside design conditions without damages. SIET has equipped the HX with a mechanical cage adequate to support the pressure in case of high temperature impact on structural resistance and with a metal shield on the access side.

Figure 20: TEMPCO TCBC2120 “out of the box” (A), installed with metallic shield (B;C) and with mechanical guard (D)

2.2.3. Data acquisition system

The ELSMOR facility's DAS is made up of National Instruments parts and SIET-developed DAS software running in NI LabView. Three chasses use DAS boards to collect low level voltage signals (± 50 mV) for TcK as well as high level voltage signals (1 : 10 V) for P, DP, and RTD. All data acquisition was done at 4 Hz frequency.

The DAS carries out the following duties:

1) Raw voltage signal acquisition;
2) Engineering unit conversion of voltage signals;
3) Conversion of engineering units in derived engineering quantities;
4) Writing of data files;

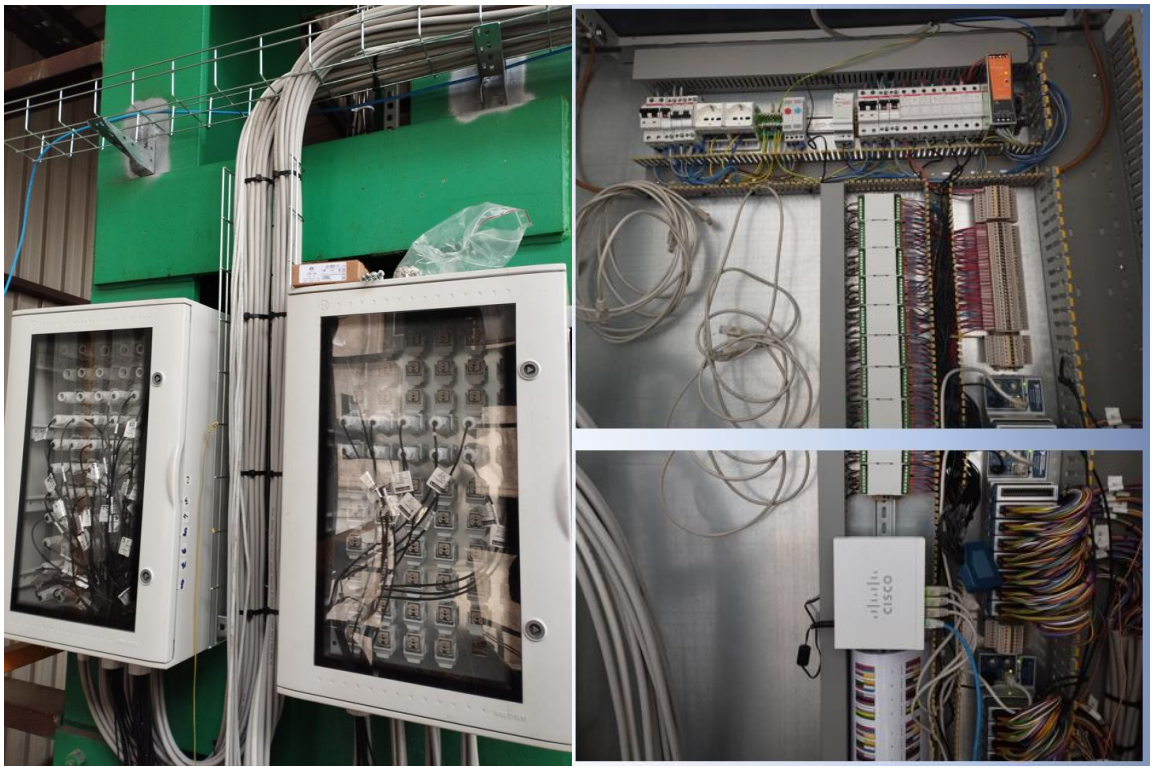

Figure 21: RTD cabling in the junction boxes (left), board cabling in the DAS frame (right)

2.3. Experimental campaign

The primary goal is to experimentally validate a Decay Heat Removal system (DHR) for the E-SMR that rejects reactor decay heat to a water pool using passive mechanisms of natural circulation. There are two heat exchangers (HX) involved: a vertical tube HX that couples the secondary side to the water pool and a plate type HX that couples the primary side to the secondary side. This type of system is thought to be the most efficient passive system available for securely managing SMR incidental and accidental situations as well as completing the long-term decay heat removal without

requiring electricity or external input. To do so, the experimental campaign focused on the following tests:

- tests at different primary side temperatures (mainly 310°C or 260 °C);
- test at different filling ratios (FR) of the secondary side (natural circulation loop), starting from 60% and decreasing till instability was reached;
- tests with different non-condensable gas (N2) quantities injected in the secondary side;
- tests with different pressure drops in the cold leg of the secondary side;
- tests with different pressure drops in hot leg of the primary side;
- tests with different levels in the HX-Pool;
- tests with different temperatures in the HX-Pool;
- tests with two-phase conditions in the primary side (steam in the Separator).

All tests were performed in steady state or quasi-steady state conditions.

The filling ration (FR) is defined as the ratio between the mass present in the secondary side (after the mass extraction) and the initial mass (full) corresponding to 125 kg.

2.3.1. Problems encountered during test campaign

Some criticalities have been noted during the ELSMOR test campaign's execution:

- The CSG output temperature occasionally displayed readings that a were lower than those from other temperature sensors close by. One explanation for this could be that because of where it was installed, a layer of condensate that was running along the tube wall deposited on the tip and displayed saturation conditions even when superheated steam was present at the CSG outlet. For this reason, the two-phase condition experiments were conducted with a slightly different RTD installation, namely with the tip slightly angled toward the steam flow. In earlier experiments, the RTD's tip was placed directly in the tube's middle.
- Problems arose when the tests with the primary side were run under two-phase condition. High pressure drops (around 2 bar) happened between the electrical heater outlet and the separator inlet in the 4-inch pipe at the originally specified primary side total flowrate (23.5 kg/s). Bubbles would start circulating inside the circuit, collecting at the top of the separator. Water began to flash in the separator and other areas of the facility as a result, making it impossible to lower the separator level to expose the CSG. Furthermore, the cavitation of the pumps was a major worry because the overall flow rate would fall to extremely low levels. Because removing water to reduce the separator level was insufficient, the only way to carry out such experiments was to lower the primary total flow in order to lessen pressure drops and prevent water from flashing. Since the electrical heater was designed to operate with extremely high flow rates of subcooled liquid, doing so required bringing it very near to its critical operating conditions. Several thermocouples were put directly on the heater's collectors

in order to have a more accurate temperature measure without permanently damaging the electrical heater, which is one of, if not the most expensive component of the entire facility.

2.3.2. Results

Excellent testing outcomes have been obtained for the ELSMOR facility's passive heat removal system. The test matrix that was run allowed for the exploration of the range of parameters that cause circulation instability as well as the verification of the system's efficacy under various operating conditions. A certain amount of heat removal is still assured even when an unstable circulation occurs at very low F.R. (15%) due to the system's generally stable and efficient operation.

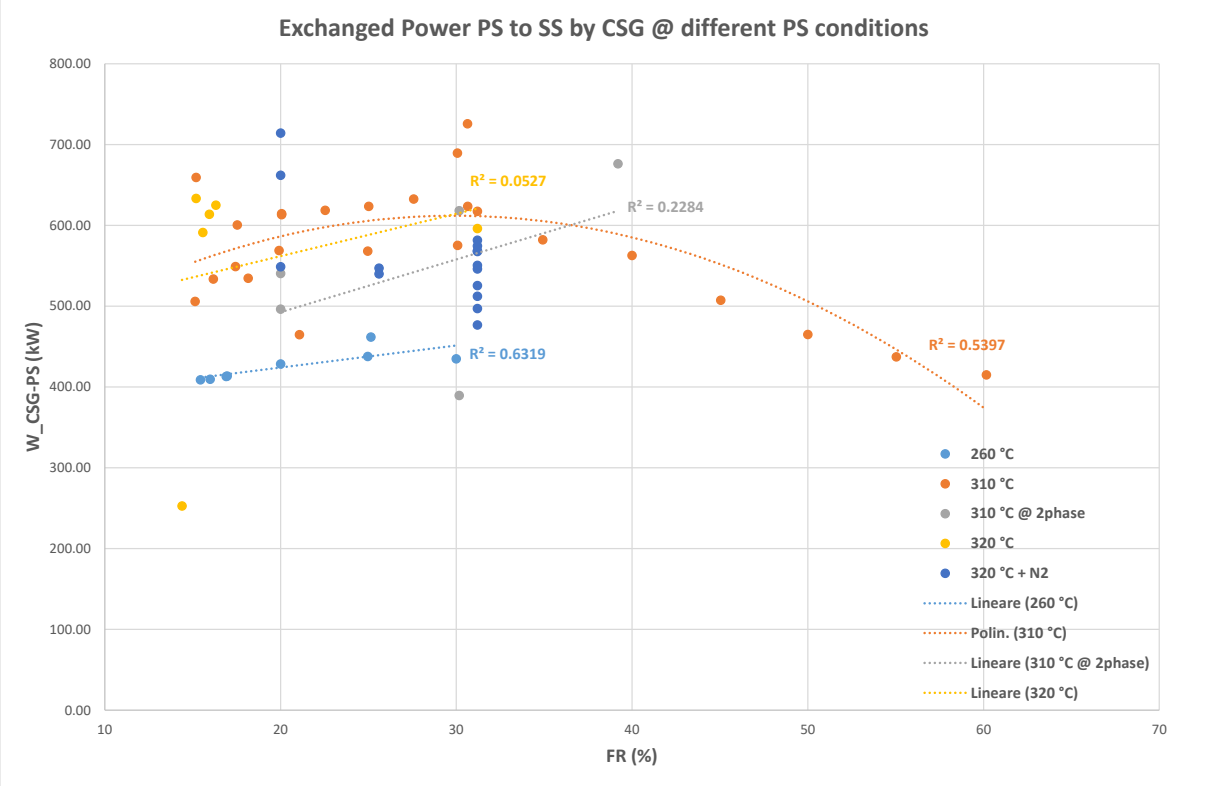

Figure 22: CSG power versus F.R. at different primary side temperatures

Filling ratio

The natural circulation and heat transfer from the primary side are significantly influenced by the filling ratio of the secondary side, one of the basic parameters.

Upon investigation of filling ratios between 60 and 14 percent, the following findings were made:

- The plant exhibits stable circulation with intermediate filling ratios (40-20%);
- The circulation becomes unstable for low filling ratios (14-15%);
- High filling ratios (60-50%) cause high pressure conditions in the secondary side, which can be hazardous to the plant's integrity.

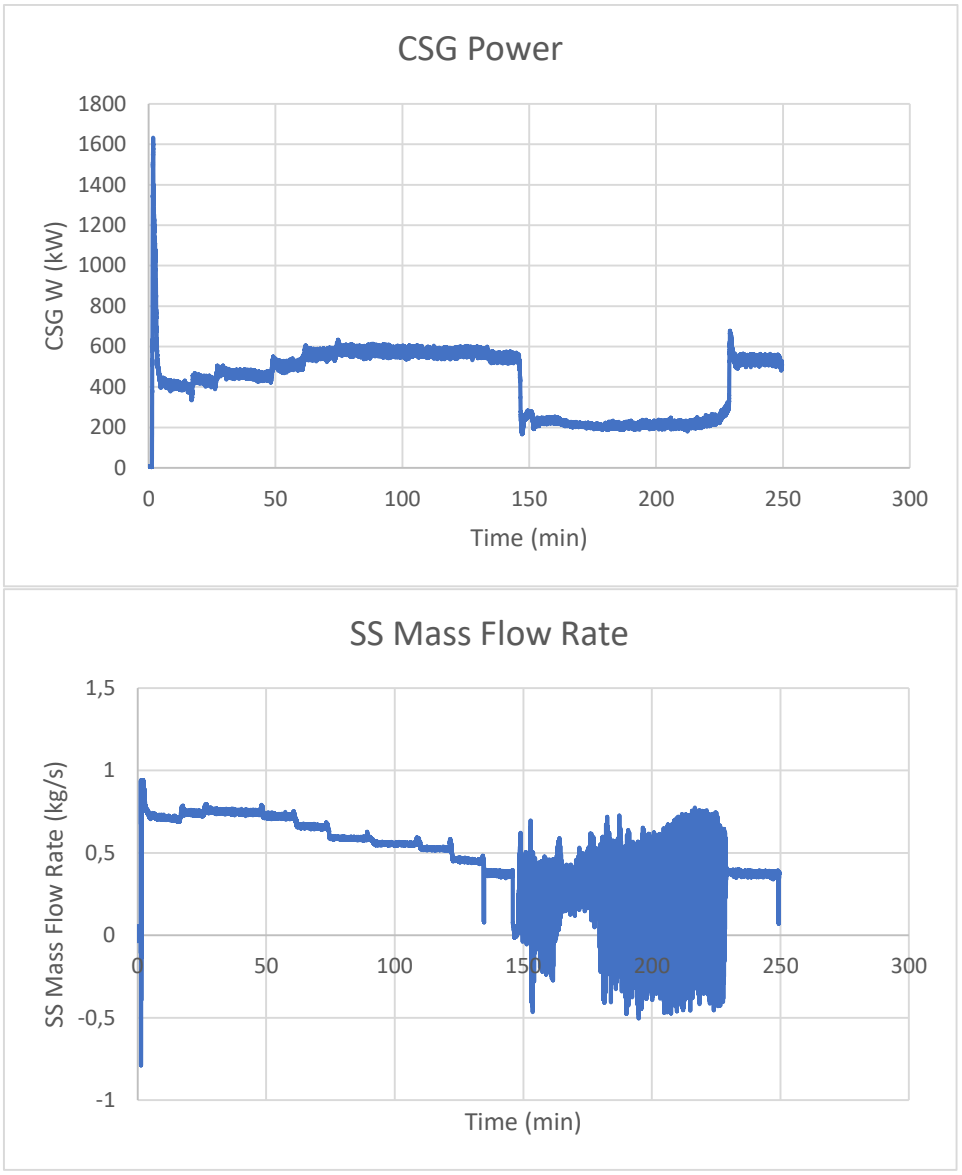

Figure 23: Time evolution of CSG exchanged power and secondary side mass flow rate. Notice the sudden drop in power occurring at FR<15% (instability zone) when the mass flow rate starts "flashing"

- The circulation exhibits hysteresis, in other words, when the F.R. is decreased, the circulation becomes unstable, and when the F.R. is increased, the circulation becomes stable at an F.R. number greater than the F.R. of destabilization. (Figure 24)

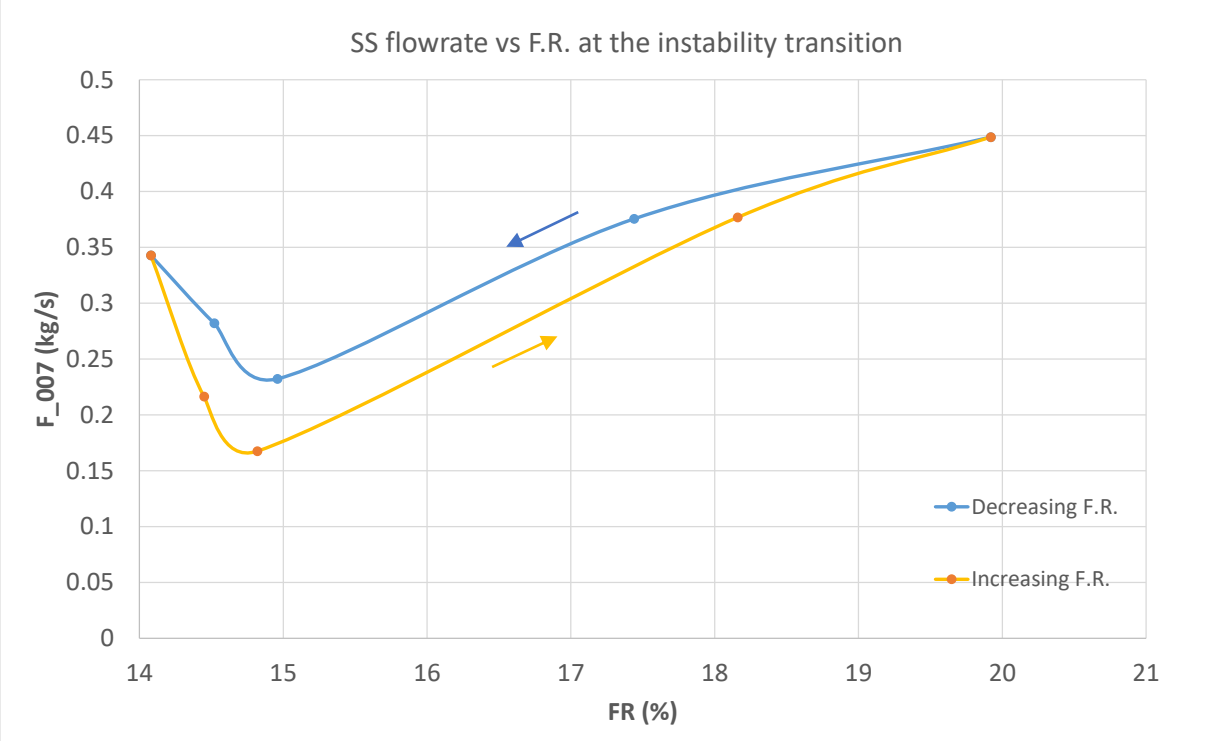

Figure 24: SS flow rate vs F.R. at the instability transition

Primary side temperature

The rate of heat transfer between the main and secondary sides is affected by the temperature of the primary side. PS temperatures between 260 and 320 °C have been investigated as indicators of various reactor main side conditions, such as those that might exist during a LOCA. At the various PS temperatures tried, the system has, overall, demonstrated stable operation.

Primary side pressure

The PS pressure is set to levels that are sufficient to fix the desired temperature, so it has little effect on how the system behaves during single-phase primary side tests. Pressure is closely correlated with temperature, which drives the heat transfer, for tests in two-phase conditions on the primary side.

Primary side flowrate

By balancing the pressure drops between the hot leg and the Separator through the flow restrictor, the main side flowrate through the CSG is determined in single-phase tests. Primary side flowrates between 3 and 4 kg/s have been investigated. Pressure also decreases as flowrate rises, but heat transfer also does. It is worthwhile to conduct tests close to the designated flowrate of 3.4 kg/s because both the main and secondary sides of the CSG naturally circulate in the reactor.

HX-Pool temperature

The vertical tube heat exchanger in the HX-Pool's water temperature determines how quickly condensation occurs there: the lower the temperature, the more heat is transferred. Temperatures in the 10 to 100 °C range for HX-Pools have been investigated. In the vast majority of tests, there was evidence of water stratification, with warmer water at the top and colder water at the bottom. The HX-Pool is topped off with cold water from the bottom to maintain the water level when mass is lost to evaporation, which is one of the reasons that contributes to stratification.

HX-Pool level

The vertical tube heat exchanger in the HX-Pool's water level determines how quickly condensation occurs there: the lower the level, the slower the heat transmission. Although HX-Pool levels between 4.5 and 2 m have been investigated, the bulk of tests have been carried out with high HX-Pool levels.

Secondary side cold leg pressure drop

The natural circulation in the loop is impacted by the pressure drops on the secondary side cold leg (between the in-Pool HX outlet and the CSG inlet). With a manual valve closed gradually, pressure reductions can be controlled. While a few tests were conducted with the valve only partially open (10/12 turns), the bulk of tests were conducted with the valve fully open. The effect on natural circulation and heat transfer rate is minimal in this position. The filling ratio has the greatest influence on circulation at constant valve location. The valve has been tested in various positions from 10/12 turns open to completely closed and back to 10/12 turns open. Only at the smallest opening of the valve—1/12 turn open—has destabilization of circulation been recorded, with quick stabilization upon valve reopening.

Non condensable gas

Only when a large amount (>1000 Nl) of non-condensable gas is injected into the secondary side does it affect natural circulation and heat transmission. The In-Pool HX's bottom header is where the non-condensable gas builds up until it fills the tubes. The In-Pool HX outlet temperature decreases as there is more gas present, which lowers the quality at the CSG outlet. Regardless, the effect on heat transmission is minimal until the filling ratio is high enough to prevent gas from reaching the CSG (Figure 25). Testing has been done on non-condensable amounts in the range of 0 to 1400 Nl.

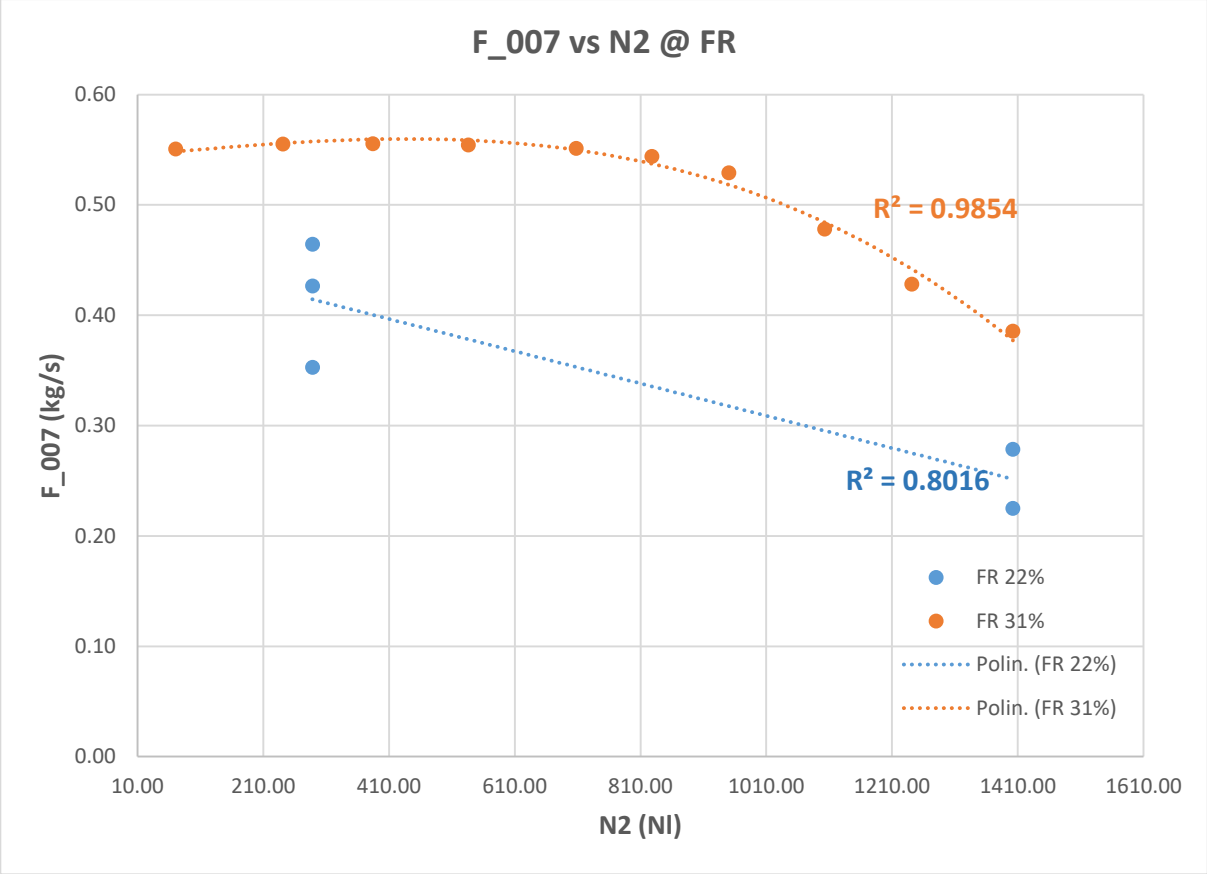

Figure 25: Secondary side flowrate versus non-condensable injected at different F.R

Primary side two-phase conditions

By keeping the Separator level below the lowest connection of the CSG, it has been demonstrated that the system can operate with steam at the primary side of the CSG (representing the reactor in an advanced phase of a LOCA transient with mass lost down to expose the S-CSG). This mode of operation is a good representation of a natural steam cycle in the primary side of a CSG that suctions as much steam as it can condense and is cooled by water flowing through the secondary side. The only way to estimate transferred power is by an energy balance at the HX-Pool, which, in any case, indicates a relatively high power confirming the good performance of the system. This is because no measurement of power can be obtained by enthalpy balance in two-phase conditions (unknown quality both primary and secondary side).

3 CSG heat transfer coefficient analysis

The following paragraphs will show a general overview of single-phase and two-phase correlations chosen among the most accredited ones. Following this there will be an in-depth explanation of the data analysis performed on SIET's data in order to characterize the heat transfer coefficient of the CSG.

3.1. State of the art of PHE single-phase correlations

In the past, great effort was put into doing experimental research on the plate heat exchanger's heat transfer properties. Statistics have been made available for many chevron and herringbone patterns and heat exchangers with wash board plates. The initial attempts in this sector date back to the latter half of the 1950s. Troupe et al.'s [9] investigation was conducted utilizing washboard-style plates and water. They may be regarded as the pioneers in the creation of correlations for plate heat exchangers. Emerson [10], employing chevron-type plate heat exchangers, may have been the first to present data on heat transfer and frictional pressure drop for laminar and transition area flows. The correlations that followed in the years were special in that they related to a particular geometry, fluid, and operational experimental range. A leading coefficient and exponent as a function of chevron angle were used in most of them, with the majority taking the shape of a power law curve fit. A PHE's improved heat transfer performance is caused by a number of improvement mechanisms that are thought to be a direct result of the plate surface properties. These include secondary circulations, vortex flows, swirl flows, and detachment and reattachment of boundary layers. It should be emphasized that the majority of the research only offer limited information on test conditions and plate geometry. [8] [11]

Muley and Manglik [12] conducted tests on the pressure loss and heat transmission in a single-phase flow. To study the chevron angle effect, they used three rectangular CPHEs with various chevron angles. In their single phase experimental research on heat transmission and isothermal frictional pressure loss, Muley and Manglik took into consideration two symmetric 30°/30° and 60°/60° degree configurations as well as a mixed chevron 30°/60° degree configuration under the conditions of Reynolds number ranging from $6 \cdot 10^2$ to 10^4. As the chevron angle increased, both the Nusselt number and the friction factor were observed to rise; however, the friction factor rose more quickly than the Nusselt number. They have reported correlations for heat transmission and pressure decrease based on experimental data.

Over a wide range of plates, Heavner [13] et al. looked into the impacts of mixed chevron angles. They conducted studies for 400<Re<10000 for b = 23°/23°, 23°/45°, 45°/45°, 23°/90°, and 45°/90°. It was discovered that the chevron angle increased with

heat transfer and pressure drop. However, their results differ significantly from other published investigations in quantitative terms.

Using experimental data and water as the working fluid, Kumar [14] and Thonon [15] proposed correlations using various coefficients based on the chevron angle and Reynolds number. The correlations' applicable ranges are $Re \leq 10^4$ and $50 \leq Re \leq 1.5 \cdot 10^4$ respectively.

Khan [11] et al. used the same three plate configurations as Muley and Manglik, with a surface enlargement factor of 1.117. Not only among all the previously mentioned literature, Khan et al. provided in great detail specifications regarding his experimental setup, but also the chevron plates geometrical characteristics were very near to the actual values of the TEMPCO heat exchanger (Table 4).

Condensation heat transfer studies with R134 using an experimental refrigerant loop a were conducted by Yan and Lin (1999) [16] in a vertical PHE with a 60° chevron angle.

Table 4: Geometric characteristics of chevron plates tested in Khan et al vs present study

	Khan et al.	**Case study**
Plate width (mm)	185	180
Vertical distance between centers of ports (mm)	565	519
Port diameter (mm)	43	50.8
Horizontal distance between centers of ports (mm)	125	92
Corrugation depth, b (mm)	2.2, 2.9, 3.6[2]	1.75
Plate thickness, t (mm)	0.5	0.4
Effective heat transfer area of plate, A (m^2)	0.095	0.095
Corrugation pitch, λ (mm)	13.25, 6.25[3]	n.a.
Surface enlargement factors, φ	1.117	1.127

3.2. State of the art of PHE two-phase correlations

Over the years, two-phase flow heat transfer has received less study than single-phase flow inside plate heat exchangers. Only a small number of studies from various research groups have been conducted in order to investigate the two-phase flow heat transfer and pressure drop mechanisms. Several empirical correlations to predict the thermal performances have also been proposed, but they have not yet been widely validated beyond their original data set, moreover smaller data sets of independently obtained data are frequently employed instead of larger ones. As opposed to single-phase heat transfer, two-phase flow is a function of a number of additional

[2] For β=60°/60°, 30°/60° and 60°/60° plate configurations, respectively
[3] For β=30° and 60° plates, respectively

thermodynamic variables, including quality, heat flux, mass flux, incipient boiling, surface structure, local flow regimes, dry out, film thickness, and oil effects.

Saturated flow boiling studies with R134a was conducted by Yan and Lin (1999) [17] in a vertical PHE with a 60° chevron angle. In-depth research was done on the influences of vapor quality, mass flow rate, heat flux, and system pressure on the evaporation heat transfer and pressure drop. They proposed a correlation to forecast their experimental heat transfer coefficient data using R134a, using the boiling number and an equivalent Reynolds number.

Khan's et al. [18] [19] experimental setup for two-phase boiling was the same as for the single-phase experiments. According to reduced pressure, equivalent Reynolds number, and boiling number, empirical correlations for a two-phase Nusselt number and Fanning friction factor have been proposed. In addition, they discovered that the equivalent Reynolds number had a substantial influence on the pressure drop whereas saturation temperature had a small impact. Depending on the chevron angle, the authors offered three distinct empirical correlations.

Park and Kim [20] investigated the heat transmission and pressure decreases of boiling R134a in a 45° shell and plate heat exchanger. Experimental research was done to determine how the measured data were affected by the mass flux, average imposed heat flux, saturation temperature, and vapor quality. They also observed that the pressure drops and evaporation heat transfer coefficients for an oblong shell and plate heat exchanger were higher than those for a plate heat exchanger, with the pressure drop increase being more apparent than the evaporation heat transfer coefficient increase. Last but not least, empirical correlations between the measured heat transfer coefficients and pressure drops and the Nusselt number and Fanning friction factor were also offered.

In a plate heat exchanger, flow boiling of water at low mass flux was examined by Lee et al [21].To achieve the appropriate heat flux, cartridge type heaters were inserted in end plates constructed of aluminum alloy. The effect of heat flow on the heat transfer and associated frictional pressure drop was insignificant, according to the research, who also linked their experimental data points to the convective boiling regime. The authors also found that, in contrast to most of the research mentioned above, the heat transfer coefficient dropped with rising vapor quality and decreasing mass flux. (Figure 26)

In the convective flow boiling regime, most of the research show that the heat transfer coefficient and the corresponding frictional pressure drop rise with vapor quality along the plate. In actuality, the refrigerant vapor quality improves during the evaporation process, increasing the specific volume and, subsequently, the fluid velocity. Because of the increased turbulence and shearing between the liquid and vapor phases caused by the greater velocity, the convective heat transfer coefficient is improved, and the frictional pressure drop that results also increases. (Figure 26)

According to the Bond number, Amalfi [22] [23] investigated the two-phase flow processes at the microscales (Bd<4) and macroscales (Bd>4) using the boiling experimental data from prior investigations, based on a dimensional and multiple regression analysis. These techniques were developed from 1903 heat transfer data points and 1513 frictional pressure drop data points, respectively, and they were demonstrated to be more accurate than any other published technique under a very diverse range of operating conditions, plate designs, and fluids (including ammonia).

As mentioned previously, the vapor quality, heat flux, mass flow rate, and system pressure are all factors that affect the evaporation heat transfer coefficient. These factors are complicated by the fact that it is unclear where the process switches from being dominated by nucleate boiling to becoming dominated by convective boiling, a transition whose threshold has not yet been accurately quantified. All the correlations presented before depend on Reynold equivalent number and Boiling equivalent number, which are functions of an averaged vapor quality.

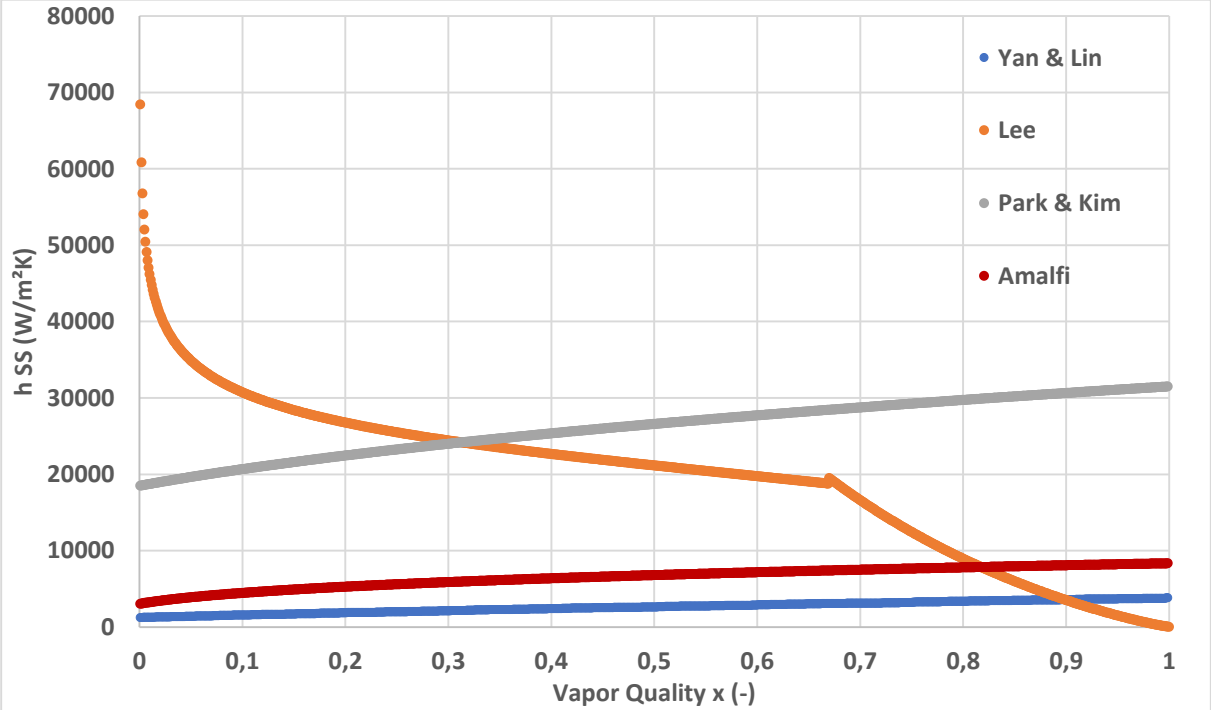

Figure 26: Sensitivity analysis of the main reviewed two-phase correlations

3.3. Data selection

To fully characterize the heat transfer capabilities of the CSG, it is necessary to study all possible scenarios. In the following work, two scenarios were studied:

- "liquid-liquid" case, in which both primary and secondary fluid are single phase liquid
- "liquid-evaporating", in which only the secondary fluid is a two-phase mixture

A large dataset, in steady state conditions, was extracted from SIET's experimental campaign. For the "liquid-liquid" study, only the datasets where the secondary fluid would primarily undergo heating rather than boiling were chosen, and for the "liquid-evaporating" analysis, only the tests where the secondary fluid was entering near saturation conditions, experiencing little heating and primarily phase shift were chosen. This is because the majority of tests showed the secondary fluid going through an initial heating and evaporation inside the CSG. This was done in order to independently investigate the contributions to the overall heat transfer coefficient made by the primary fluid (liquid, single-phase water) and the secondary fluid (single or two-phase water). Two and three data sets, respectively, were discovered to fit these requirements, and Table 5 lists the operational parameters.

Table 5: Steady state conditions of the selected experiments

	LIQUID - LIQUID		LIQUID - EVAPORATING		
FR (%)	60.16	55.04	30.08	19.92	17.44
PS inlet T (°C)	310.76 ± 0.99	311.78 ± 0.99	310.88 ± 0.99	310.64 ± 0.99	310.73 ± 0.99
Power exchanged (kW)	415.04 ± 0.12	437.22 ± 0.15	575.39 ± 0.16	568.99 ± 0.16	549.01 ± 0.15
PS mass flow rate (kg/s)	3.49 ± 0.37	3.48 ± 0.37	3.58 ± 0.38	3.59 ± 0.38	3.61 ± 0.38
SS mass flow rate (kg/s)	0.72 ± 0.01	0.74 ± 0.01	0.56 ± 0.01	0.45 ± 0.01	0.38 ± 0.01
PS Pressure (MPa)	11.71 ± 0.006	11.93 ± 0.006	11.92 ± 0.006	11.92 ± 0.006	11.92 ± 0.006
SS Pressure (MPa)	9.33 ± 0.012	9.15 ± 0.012	6.45 ± 0.012	5.99 ± 0.012	5.83 ± 0.012
SS inlet T (°C)	187.01 ± 0.64	200.42 ± 0.64	266.29 ± 0.64	272.62 ± 0.64	272.66 ± 0.64
SS saturation T (°C)	305.91	304.50	280.35	275.52	273.76
W heating (%)	98.24	85.57	7.01	1.17	0.38
Overall HTC Uexp (W/m²K) [4]	1069.37 ± 202.79	1098.23 ± 154.24	2135.53 ± 234.42	2402.36 ± 368.21	2139.09 ± 295.39

[4] The CSG global heat transfer coefficient was calculated with the LMTD method.

3.4. Single-phase model validation with TEMPCO data

In response to SIET's request, TEMPCO analyzed four potential PHE operational scenarios and estimated the overall heat transfer coefficient and the fluid specific heat transfer coefficient for each. These scenarios were: symmetric[5] liquid-liquid, liquid-evaporating, liquid-superheated steam and evaporating-evaporating.

Starting with the liquid-liquid condition, the initial strategy was using TEMPCO's input parameters to validate the single phase correlations that had previously been provided. By selecting the model that produced an output h_{1p} that was closest to the value discovered by TEMPCO, it was feasible to determine which model was the most appropriate. In order to fit the global heat transfer coefficient $(U_{\exp})$, which was obtained from the experimental data gathered by SIET, a "theoretical" two-phase heat transfer coefficient (h_{2p}) was evaluated for the liquid-evaporating case. After examining a number of two-phase correlations using the experimental data, the one that matched the "theoretical" correlation the closest was selected. Unfortunately, this approach didn't lead to desirable outcomes. The following are the key findings that were noted.

- **Liquid-Liquid**: By using the data from TEMPCO, Heavner, Thonon and Kumar produced the closest h_{1p} to the $h_{1p}$of TEMPCO, but when using the data from SIET, they produced a U_{model}that was three to four times greater than the U_{exp}. Yet, Muley & Manglick produced a U_{exp}that was extremely comparable to U_{exp} values while producing a h_{1p}that was almost a third smaller than TEMPCO's h_{1p}. As a result, while Heavner, Thonon, and Kumar correctly forecast the $h_{1p}$of the primary fluid (whose operational conditions are very similar to those of the symmetric case of TEMPCO), they overestimate the contribution of the h_{1p} of the secondary fluid, which increases the value of U_{model}. Instead, Muley and Manglick estimated the secondary fluid's h_{1p} with a high degree of accuracy. Overall, all of them overestimated the heat transfer coefficient as shown in Figure 27.

[5] Primary and secondary fluids working under same pressure of 120 bar and having same mass flow rate of 3,5 kg/s

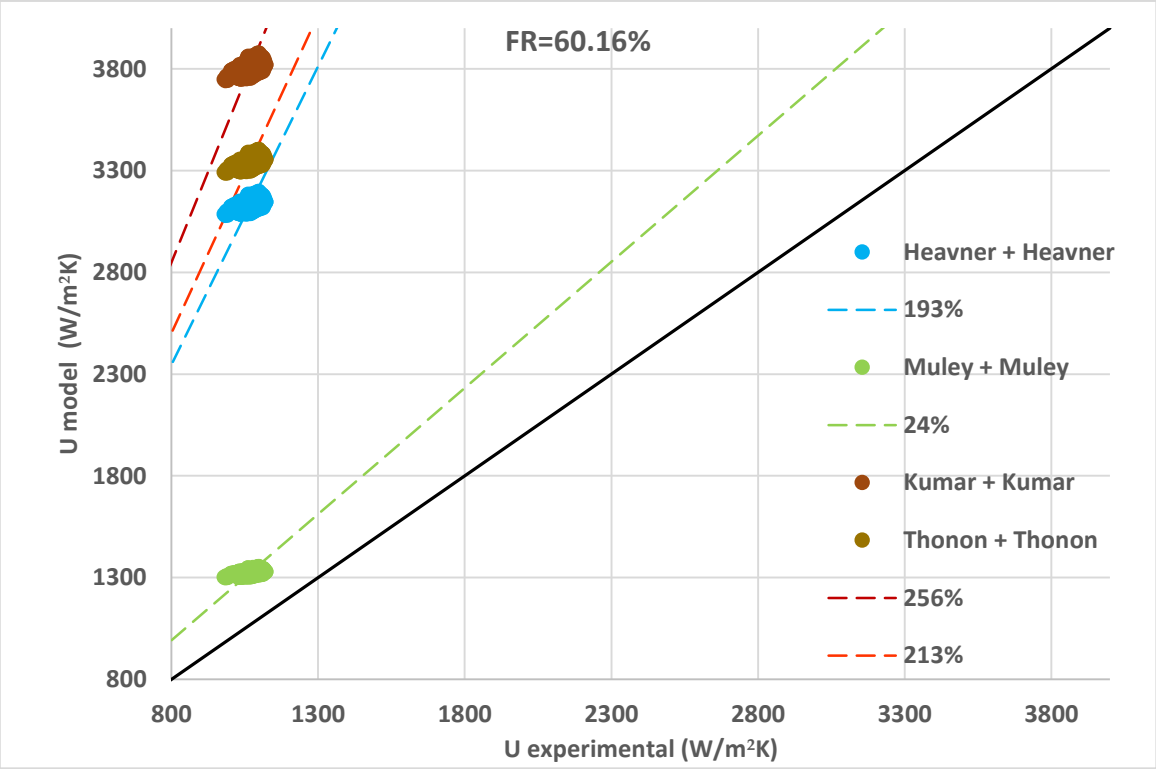

Figure 27: Evaluation of correlations for single-phase heat transfer for FR=60.16%. Similar results are obtained also for the FR=55.04%. The trend lines are prediction performance of the corresponding correlation calculated with the root mean square error (RMSE)

- **Liquid-Evaporating**: Knowing the U_{exp} and using for example Heavner as the main correlation for single-phase convective heat transfer (the expected h_{2p} was calculated as follows:

$$h_{2p_{expected}} = \left(\frac{1}{U_{exp}} - \frac{1}{h_{1p}} - \frac{t_{plate}}{k_{plate}}\right)^{-1}$$

Yan & Lin were therefore shown to get the most accurate results among the examined two-phase correlations by applying this logic. When comparing different data sets, this correlation combination didn't always get the best outcomes. Figure 28 demonstrates that Muley & Manglick + Yan & Lin is consistently outperformed by all other combinations while maintaining Yan & Lin as a two phase correlation. This is most likely a result of Muley & Manglick's poor ability to predict the behavior of the primary fluid. On the other hand, single phase predictions that were previously disregarded now perform better than all the other combinations by a small margin. (Figure 29)

In conclusion, it is challenging to come up with a combination that works in all situations due to the correlations' inconsistent predictions (both single and two phase). As a result, the following step is to develop an ad hoc correlation for this particular plate CSG.

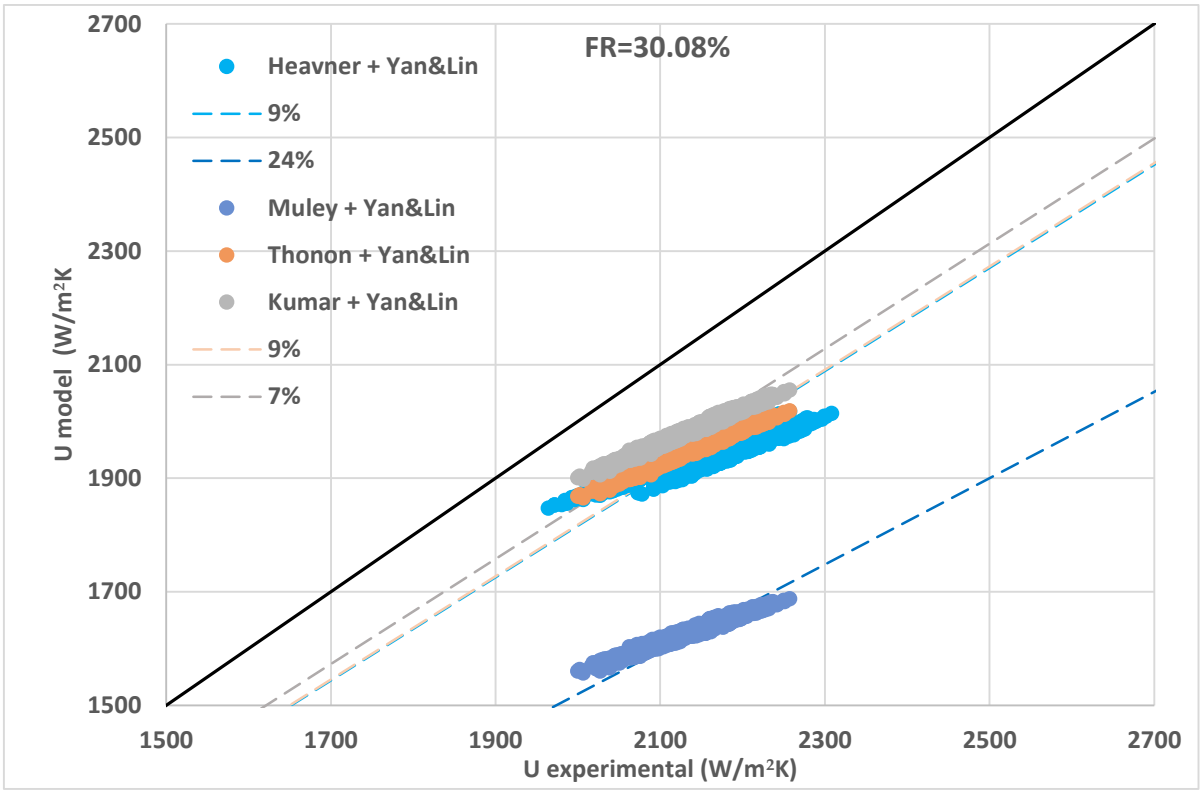
FR=30.08%
Heavner + Yan&Lin
9%
24%
Muley + Yan&Lin
Thonon + Yan&Lin
Kumar + Yan&Lin
9%
7%
U model (W/m²K)
U experimental (W/m²K)
2700
2500
2300
2100
1900
1700
1500
1500
1700
1900
2100
2300
2500
2700

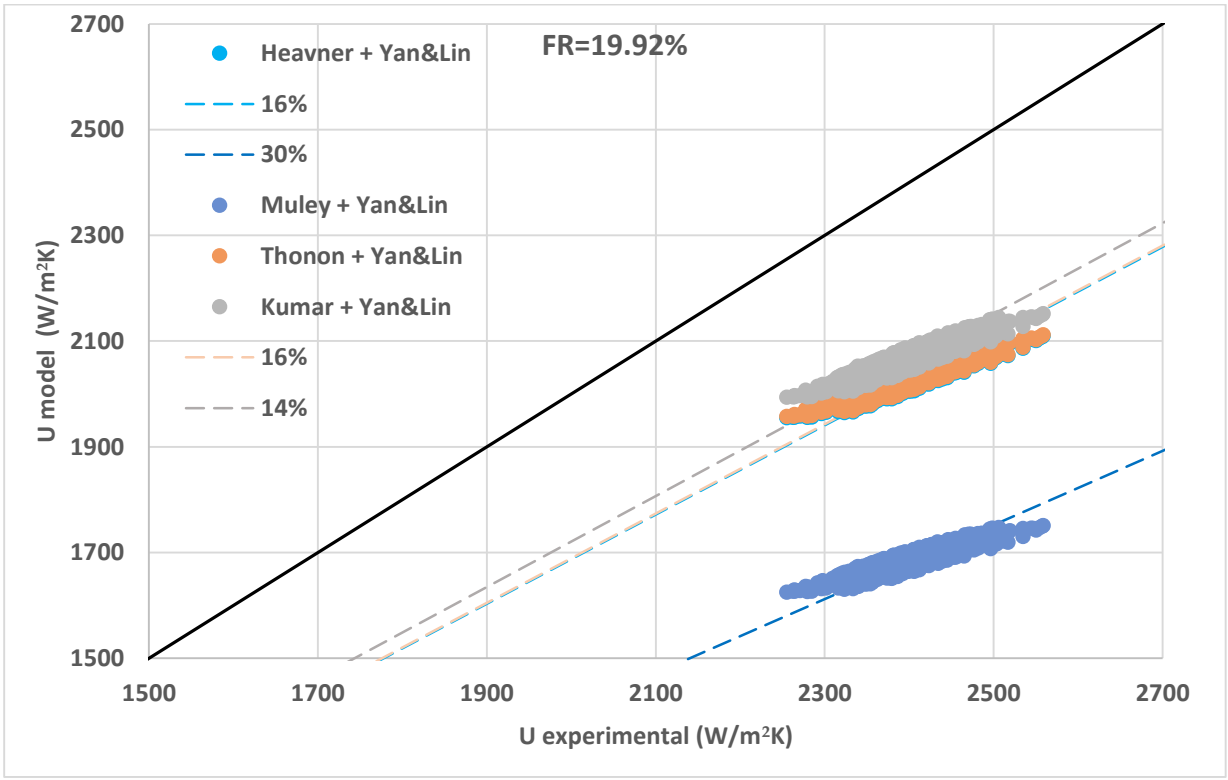
FR=19.92%
Heavner + Yan&Lin
16%
30%
Muley + Yan&Lin
Thonon + Yan&Lin
Kumar + Yan&Lin
16%
14%
U model (W/m²K)
U experimental (W/m²K)
2700
2500
2300
2100
1900
1700
1500
1500
1700
1900
2100
2300
2500
2700

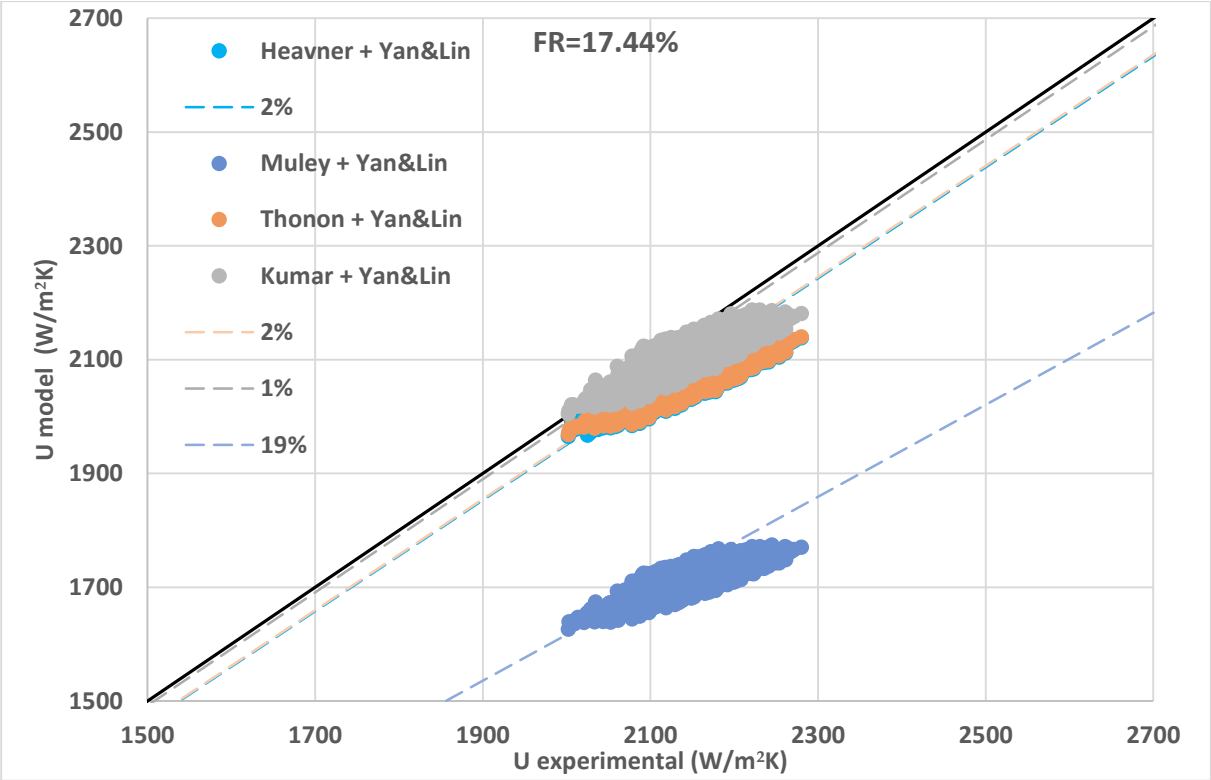

Figure 28: Evaluation of different combination of single and two phase correlations at FR=30%, 19.92% and 17.44% respectively

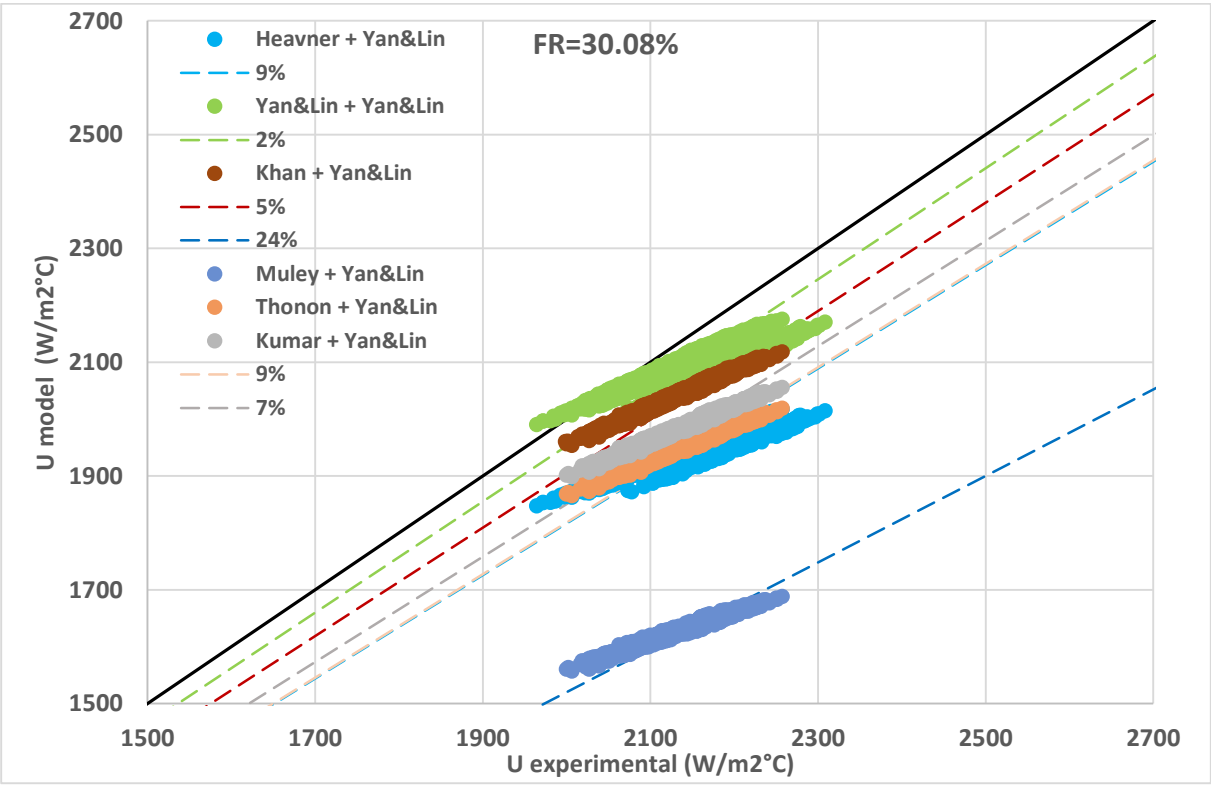

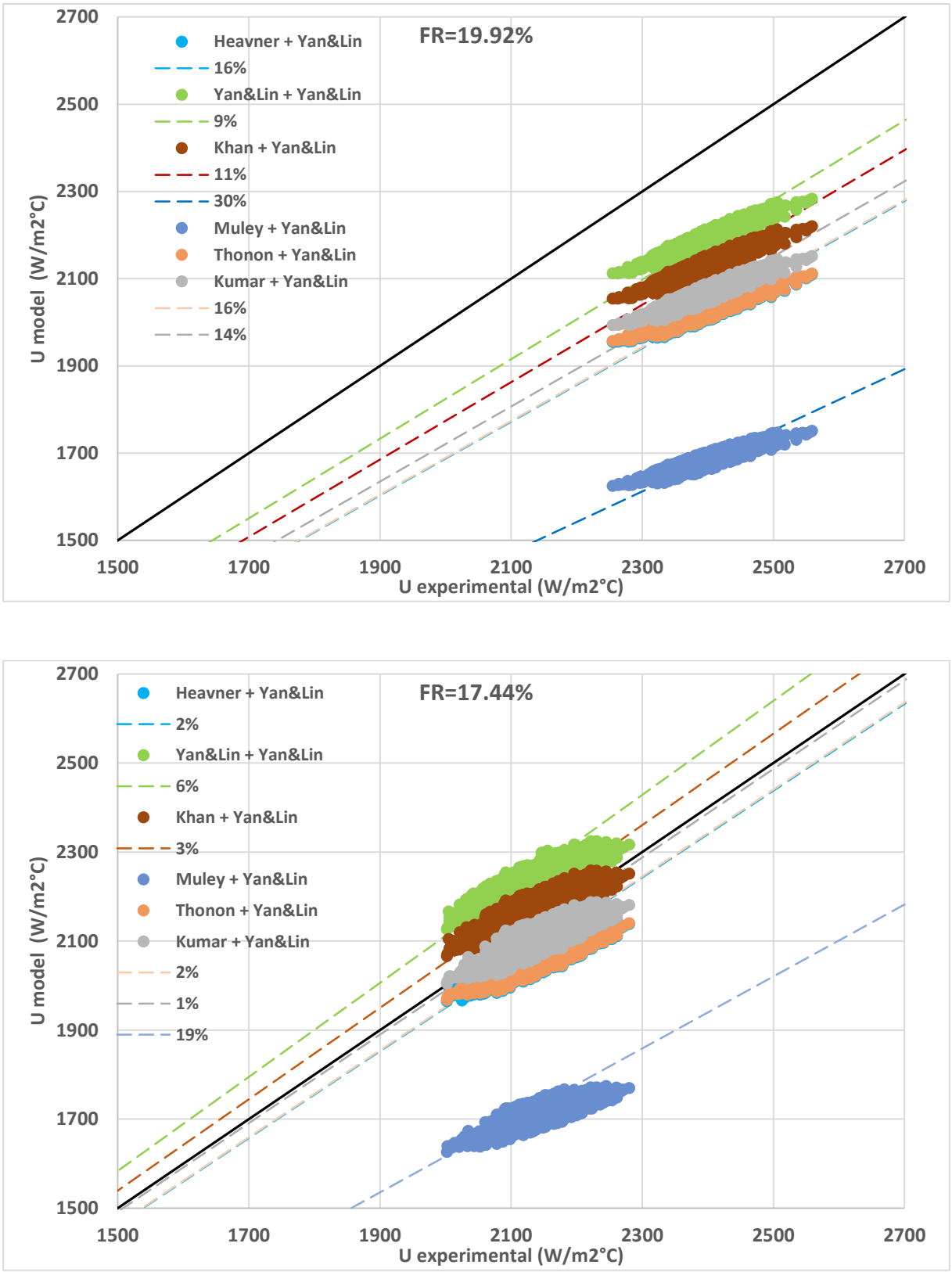

Figure 29: Evaluation of different combination of single and two phase correlations at FR=30%, 19.92% and 17.44% respectively

3.5. New correlation fitting

In the following chapters, only data from the liquid-liquid case at FR=60.16% has been used for the single phase evaluations, while for the two phase only data coming from the liquid-evaporating at FR=17.44%. These two sets were chosen among the five identified because they are the most reliable. The FR=60.16% has the highest heating power contribution (around 98%) compared to FR=55.04% (Table 5), while FR=17.44% was chosen over FR=19.92% because among the two, it has the highest vapour exit quality (around 93%).

3.5.1. Single-phase

As mentioned previously, most of the single phase correlations follow a power law curve like the following:

Equation 1

$$Nu = C(\beta, \phi) * Re^{m} * Pr^{p} * \left(\frac{\mu}{\mu_w}\right)^{k}$$

To make Equation 1 simpler, some hypotheses were introduced. Since dealing with water, Pr and μ were assumed constant values. Moreover, after reviewing the literature on plate heat exchangers with similar β and Re, the m coefficient usually adopts values around 0,70. Finally, it follows:

Equation 2

$$Nu = C * Re^{0,7}$$

Where C is a parametric constant that contain all the information regarding the plate geometry (β and ϕ). A first approach was fitting this correlation (Equation 2) in Equation 3 to get the C using the knowledge about $h_{TEMPCO} = 13512\ W/m^2K$

Equation 3

$$h_{TEMPCO} = C * Re^{0,7} * \frac{k}{d_h} \Longrightarrow C = 0,17$$

Unfortunately the resulting correlation (Equation 3), when used to calculate $h_{1P_{SS}}$ and U_{model} would yield overestimated results.

An alternative solution was to fit the Equation 2 into Equation 4 using SIET's data at FR=60.16%:

Equation 4

$$U_{exp} = \left(\frac{1}{C * Re_{ps}^{0,7} * \frac{k_{ps}}{d_h}} + \frac{t_{plate}}{k_{plate}} + \frac{1}{C * Re_{ss}^{0,7} * \frac{k_{ss}}{d_h}}\right)^{-1} \Longrightarrow C = 0,057$$

Therefore

Equation 5

$$h_{1p} = Nu * \frac{k}{d_h} = 0{,}057 * Re^{0{,}7} * \frac{k}{d_h}$$

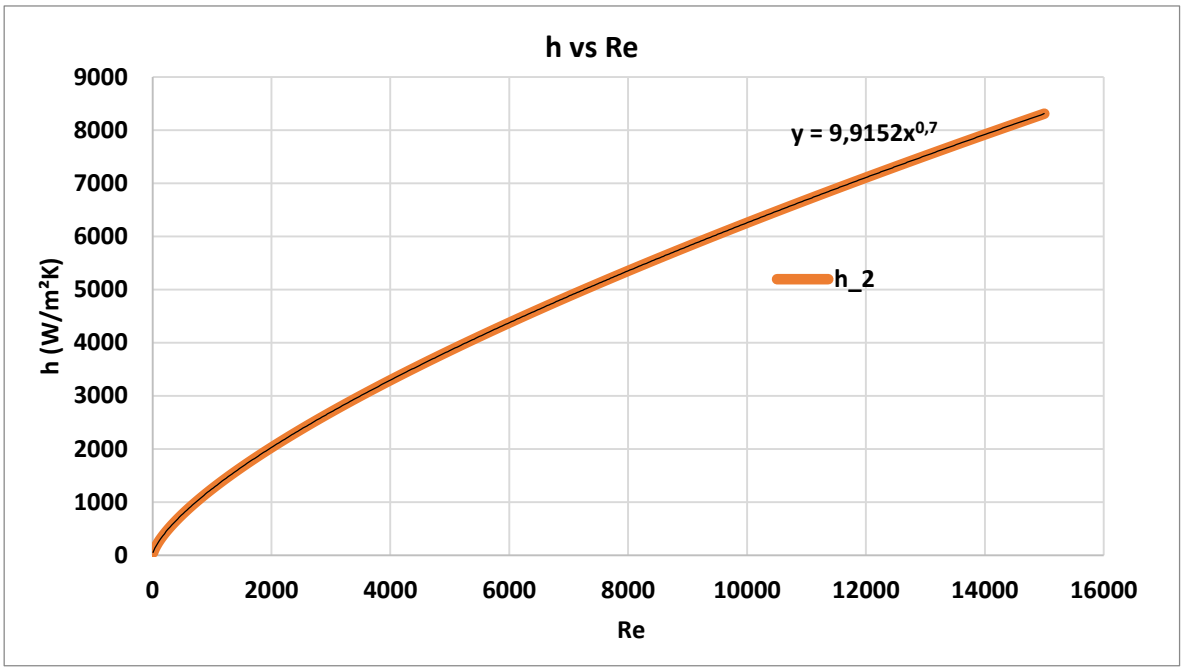

Figure 30: Newly found correlation plotted against Re

3.5.2. Two-phase

Solotych et al. [24] conducted an experimental campaign to measure local heat transfer coefficients at different configurations (60°/60° and 65/65°) using infrared thermography. The test fluid was a refrigerant (HFE7100) at mass fluxes between 25 and 100 kg/m²s, and qualities from 0 to 0.9. The apparatus and data reduction technique were validated by comparing the single-phase heat transfer and pressure drop data against the prediction methods from the literature.

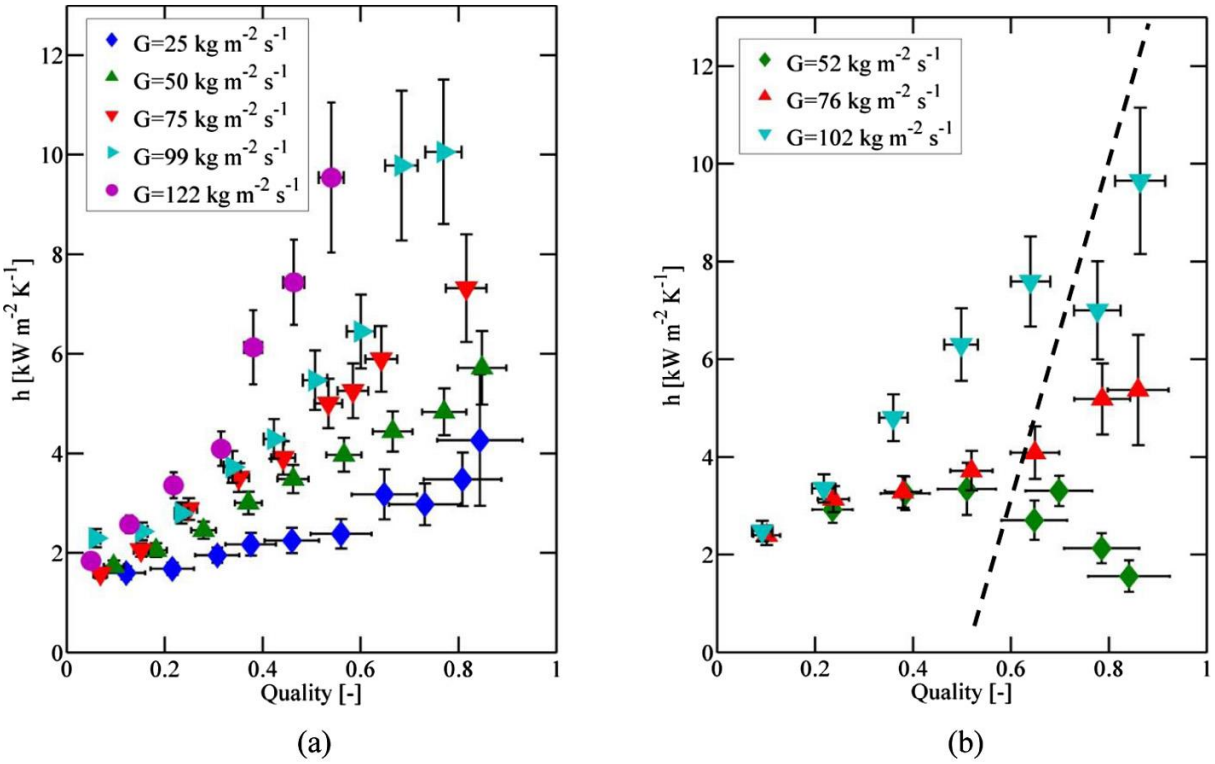

Figure 31: Results of the average two-phase heat transfer: (a) HTC for L5.7A1.0B60-60, (b) HTC for L3.7A0.5B65-65. The data to the right of the dotted line experienced dryout and are therefore untrustworthy.(Solotych et al) [24]

The two-phase HTC for both geometries is plotted against the mean quality in Figure 31. For the data when dryout does not occur, HTC rose as quality and mass flux increased for both geometries. The mass flux had little impact on HTC at low qualities, but as quality increased, the impact of the mass flux increased. Moreover, Amalfi et al. [23] conducted a sensitivity analysis (Figure 32) in order to highlight the influences of geometry on the performance of PHE.

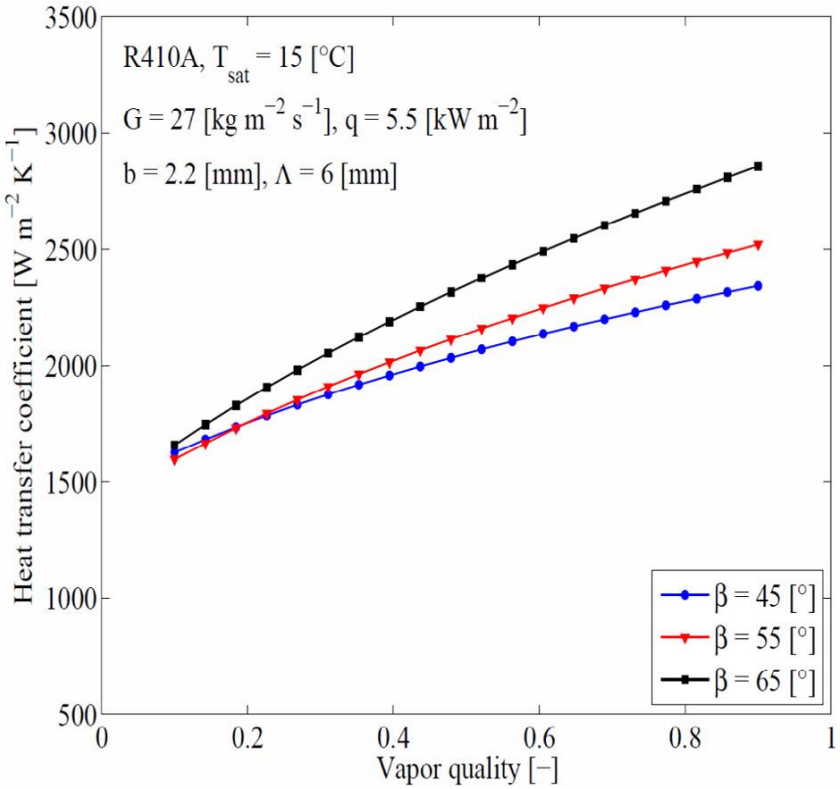

Figure 32: Sensitivity analysis on the effect of chevron angle on heat transfer coefficient using the correlations proposed by Han et al. (Amalfi et al.) [23]

With this added knowledge, knowing that PHE has a chevron angle of 45° and in the liquid-evaporating case works with low max fluxes between 18 and 27 kg/m²s, the following hypothesis can be made:

- Dryout doesn't occur in the PHE
- For low mass fluxes, a linear dependency between vapour quality and heat transfer coefficient is assumed

Therefore, the secondary fluid heat transfer coefficient is obtained by the linear extrapolation of the line passing by two known points (Figure 33):

- the single phase secondary inlet $h_{1p_{SS}}$ at $x_{in} = 0$
- the average $h_{2p_{SS}}$ at $x_{avg} = 0.465$

Equation 6

$$h_{2p_{SS}} = \left(\frac{1}{U_{exp}} - \frac{1}{h_{1p_{PS}}} - \frac{t_{plate}}{k_{plate}} \right)^{-1}$$

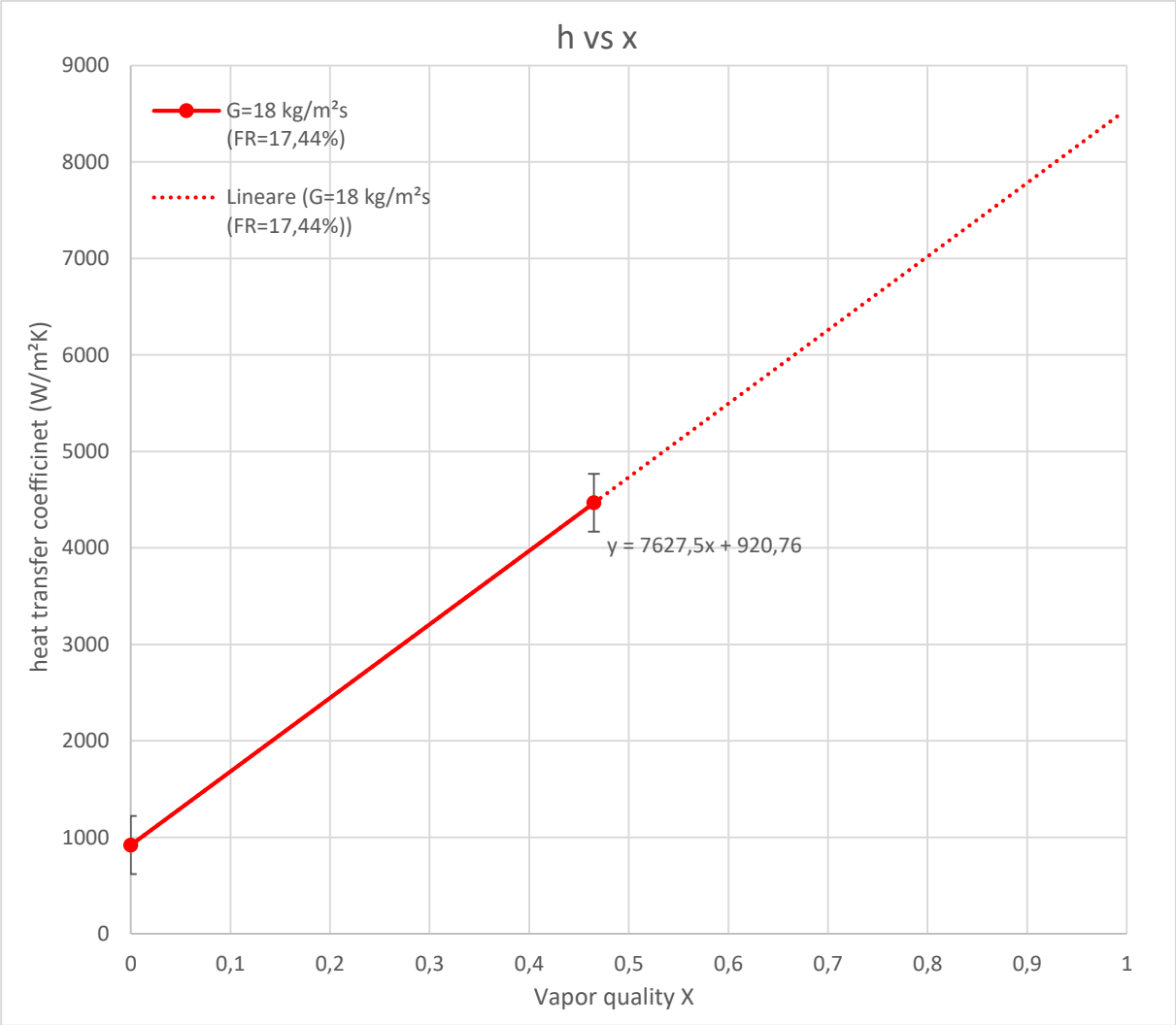

Figure 33: CSG two phase heat transfer prediction in function of vapor quality

In conclusion, thanks to experimental data and to past literature, two new correlations describing the heat transfer phenomena in single phase and in two phase were created:

Equation 7

$$h_{1P} = Nu * \frac{k}{d_h} = 0{,}057 * Re^{0,7} * \frac{k}{d_h}$$

$$h_{2P} = 7627{,}5 * x + 920{,}76$$

Unfortunately, they are unable to accurately estimate when tested on a data set at FR=45% (a mixed situation where the total power exchanged was split between subcooled heating and evaporation). Results indicate that only to exchange the total power, a heat transfer surface roughly twice as large as the nominal one should be required. A new approach is therefore needed.

3.5.3. A new approach

Table 6: Steady state average conditions of selected data

	LIQ-LIQ	LIQ-EVA	LIQ-MIX
FR (%)	60.16	17.44	45
PS inlet T (°C)	310.76 ± 0.99	310.73 ± 0.99	310.82 ± 0.99
PS outlet T (°C)	289.42 ± 0.64	283.25 ± 0.64	284.35 ± 0.64
Power exchanged (kW)	415.04 ± 0.12	549.01 ± 0.15	507.34 ± 0.15
PS mass flow rate (kg/s)	3.49 ± 0.37	3.61 ± 0.38	3.45 ± 0.37
SS mass flow rate (kg/s)	0.72 ± 0.01	0.38 ± 0.01	0.72 ± 0.01
SS inlet T (°C)	187.01 ± 0.64	272.66 ± 0.64	227.66 ± 0.64
SS outlet T (°C)	305.75 ± 0.99	273.74 ± 0.99	293.41 ± 0.99
SS saturation T (°C)	305.91	273.76	293.42
W heating (%)	98.24	0.38	47
Overall HTC Uexp (W/m²K) [6]	1069.37 ± 202.79	2139.09 ± 295.39	

Liquid - Liquid

Recalling the base scenarios in Table 6, the liquid-liquid case at FR=60,16% was first analyzed. As before, the primary HTC values used was same as TEMPCO's HTC ($h_{1P_{PS}} = 13512\ W/m^2K$). This hypothesis was then used to calculate the secondary HTC ($h_{1P_{SS}} = 1200\ W/m^2K$) necessary to get the same value of global HTC ($U_{calculated} = 1072\ W/m^2K$) as the one obtained during the experimental campaign ($U_{exp} = 1069\ W/m^2K$). The heat transfer surface required to exchange a given power step (20 kW) was estimated using the corresponding fluids HTC as a starting guess until the value of the total power was achieved (415 kW in this case). Thus, the temperature trends were retrieved as depicted in Figure 34: Temperature trends inside the CSG for primary single phase water (blue) and secondary single phase water (orange), and as is to be expected, the smaller area required to exchange a fixed value of power is caused by the bigger temperature differential between the primary and secondary fluid. Once convergence between the calculated total surface and the actual surface was attained, the secondary HTC was updated. In order to exchange 415 kW in 12,16 m², an $h_{1P_{SS}} = 1320\ W/m^2K$ was derived.

[6] The CSG global heat transfer coefficient was calculated with the LMTD method.

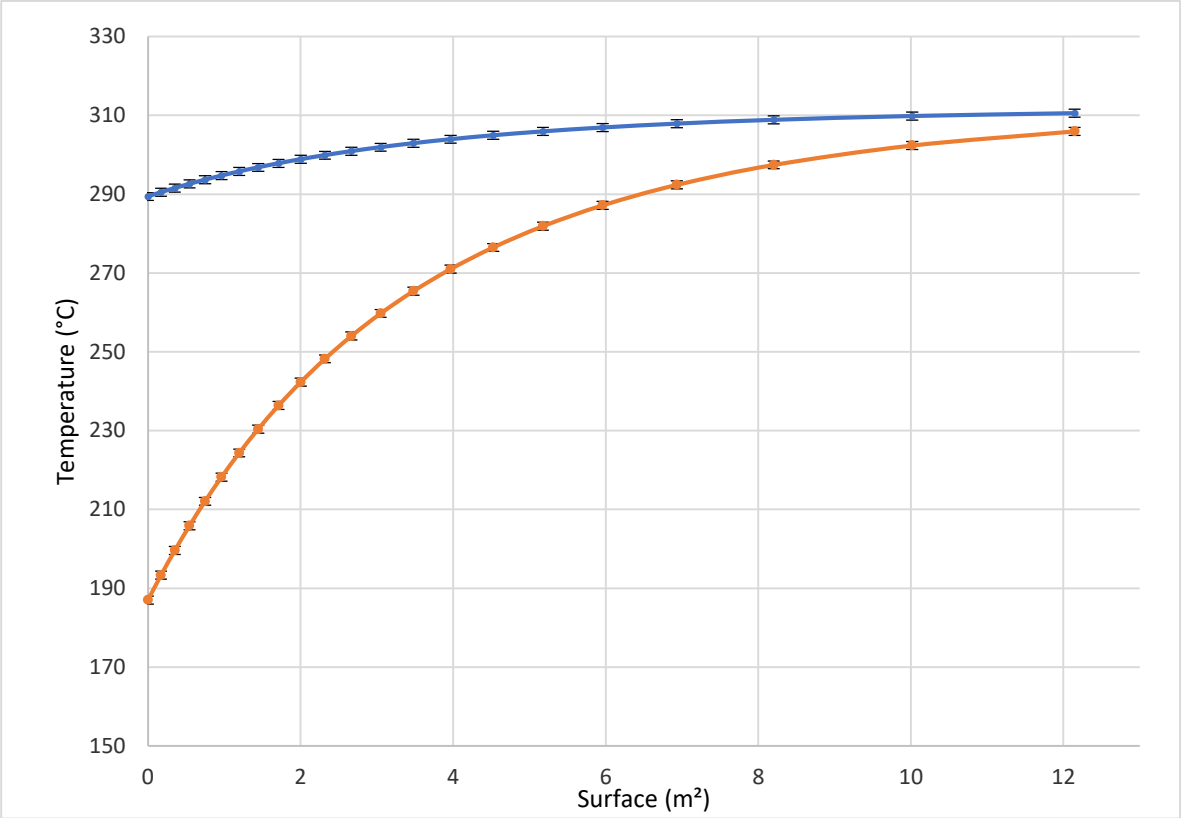

Figure 34: Temperature trends inside the CSG for primary single phase water (blue) and secondary single phase water (orange)

Liquid - Evaporating

The liquid-evaporating situation at FR=17,44% was subsequently addressed using the same methodology. Given that the mass flow rate and HTC are proportional and that the secondary mass flow rate was roughly half that of the preceding case, $h_{1P_{SS}} = 700\,W/m^2K$ was a plausible initial guess. Following that, the two phase HTC correlation, a function of the vapour quality x, is created using this beginning value. For the following correlation, convergence was attained on the heat transfer surface.

This preliminary analysis of the base cases was needed in order to confirm both Tempco's and SIET's data reliability before moving on the subsequent case.

Equation 8

$$h_{2P_{SS}} = h_{1P_{SS}} + x * h_{sat,vap} = 700 + x * 9500$$

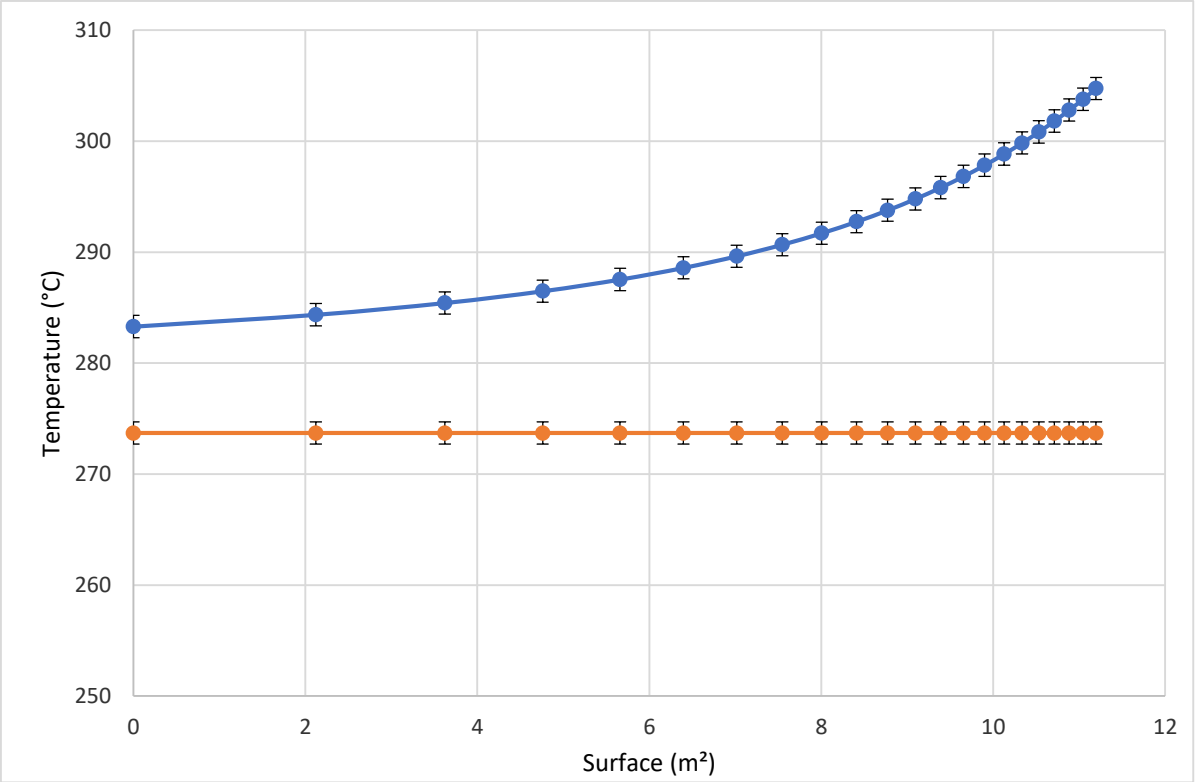

Figure 35: Temperature trends inside the CSG for primary single phase water (blue) and secondary two phase water (orange)

Liquid - Mixed

The total exchanged power for the case at FR=45% had to be divided and its two distinct contributions—one for heating the secondary subcooled water up to saturation conditions, and the other for the partial evaporation—studied separately. In fact, although the outlet vapor quality in the prior case—used as a typical reference for liquid-evaporating heat exchange—was 93%, indicating a nearly full evaporation, the outlet vapor quality in this case was only 26%. A preliminary attempt produced inaccurate results similar to those from previous attempts, in that 12 m² of surface area was required to exchange 237 kW of power (for heating) and 270 kW of power (for evaporation), which is equivalent to double the total CSG heat surface. Therefore, nucleate boiling was explored as a possible explanation for such disparities. Additionally, at 7 m², the primary temperature is higher than the secondary saturation temperature. The threshold was set at +3 °C above saturation temperature.

Since the mass flow rate has doubled compared to the liquid-evaporating example, the secondary HTC in single phase circumstances is therefore $h_{1P_{SS}} = 1320\ W/m^2K$ until the conditions of nucleate boiling are attained, at which point the secondary HTC becomes

Equation 9

$$h_{1P_{SS}(ONB)} = h_{1P_{SS}} + h_{x=0,26} = 5600\ W/m^2K.$$

This results in a surface requirement of 7,8 m².

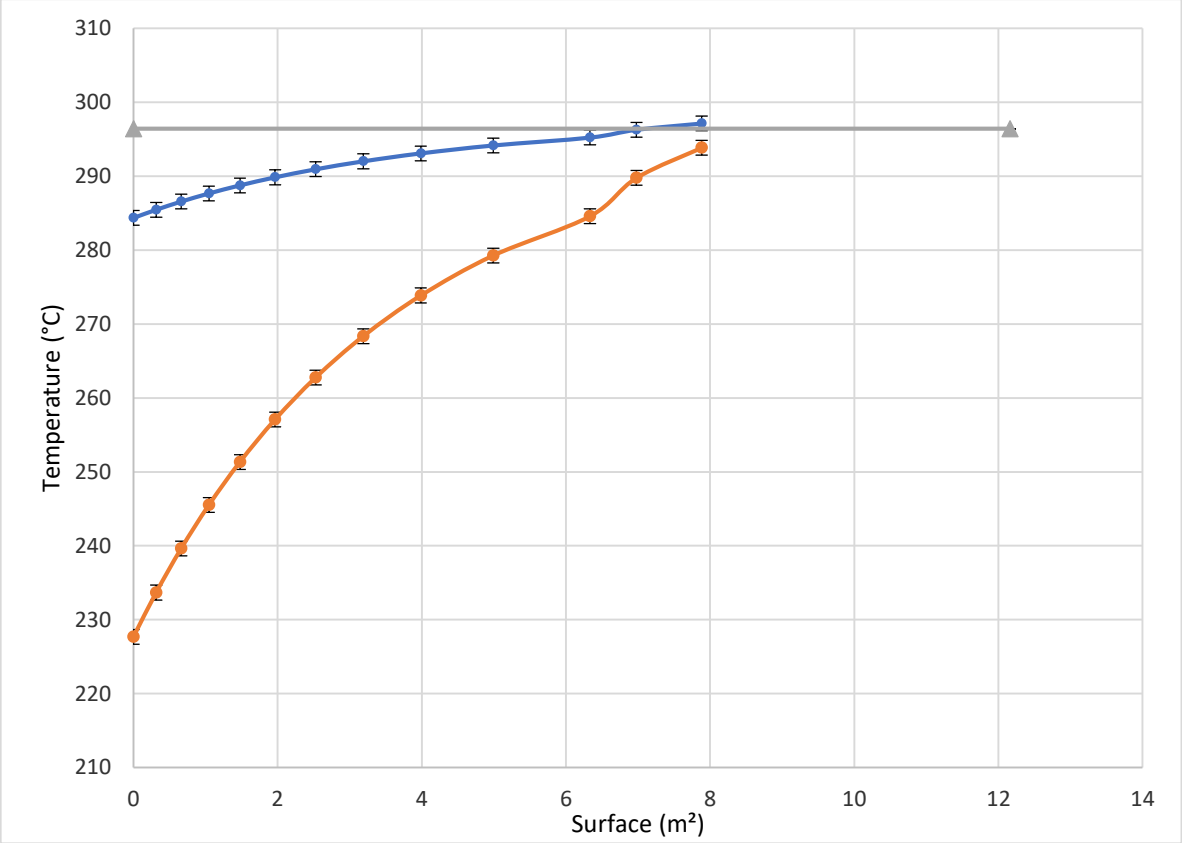

Figure 36: Temperature trends inside the CSG for primary single phase water (blue) and secondary single phase water (orange) and secondary saturation temperature (grey)

As previously mentioned, the secondary HTC in two-phase conditions depends linearly on the vapor quality as shown in

Equation 9 with initial conditions at $h_{1P_{SS}(ONB)}$. The remaining surface was then covered by fitting the value of the $h_{sat,vap}$.

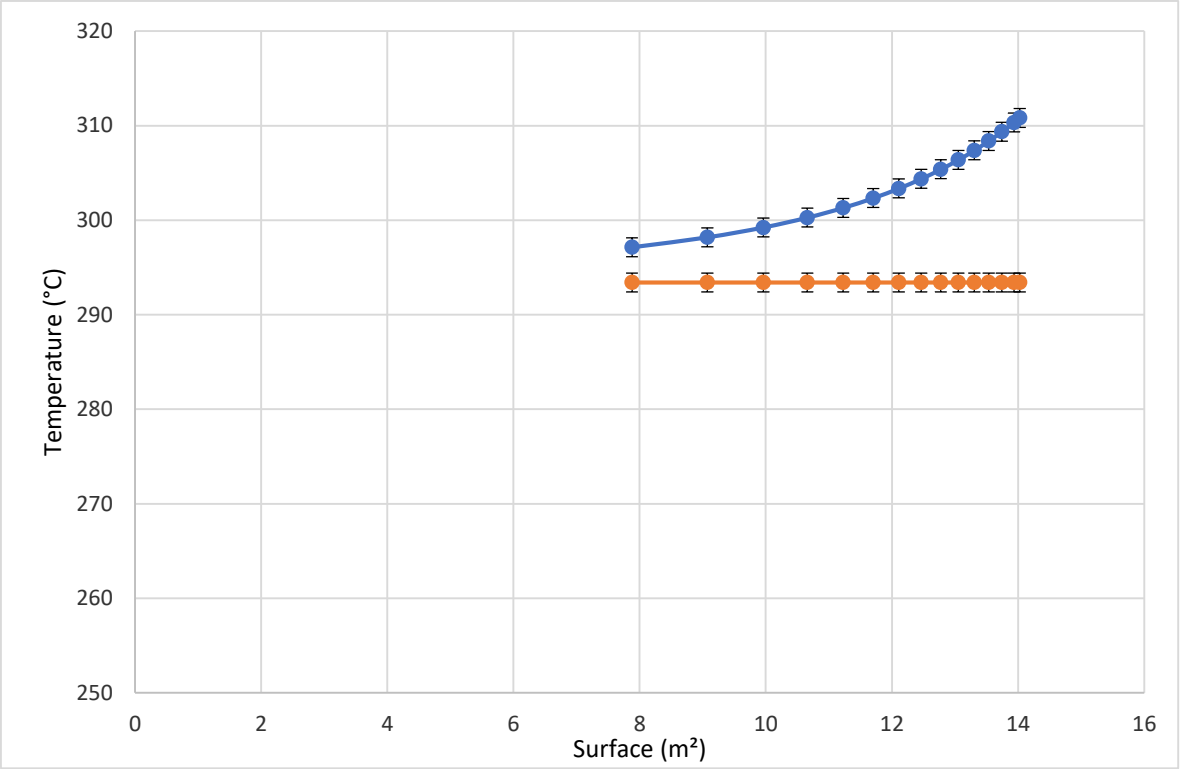

Figure 37: Figure 38: Temperature trends inside the CSG for primary single phase water (blue) and secondary single phase water (orange)

This leads to the following Equation 10

Equation 10

$$h_{2P_{SS}} = h_{1P_{SS(ONB)}} + x * h_{sat,vap} = 5600 + x * 45000$$

The necessary surface is approximately 6,15 m², resulting in a combined total surface of 14,03 m² with a 15% overestimation error.

3.5.4. Sensitivity analysis of main parameters

In the following chapter are shown graphs depicting the impact of input parameters on the CSG surface need to exchange power. All are referred to the case scenario at FR=45%, and the contribution of the liquid-liquid side is separated from the contribution of the liquid-evaporating side.

- Secondary HTC in analyzed in an interval of ± 30% from its nominal value
- Primary and secondary mass flow rates are analyzed in a ± 20% from their nominal value
- Input and output temperatures are studied in a ± 1 °C (around ± 0,01%) from their nominal value

Heat Transfer Coefficient

As shown in Figure 39, the presence of nucleate boiling is beneficial since it decreases the surface needed to exchange the same amount of power, but varying degrees of

nucleate boiling don't affect as much. Same can be said about Figure 40, in which is $h_{1P_{SS}(ONB)}$ has a bigger impact than $h_{sat,vap}$.

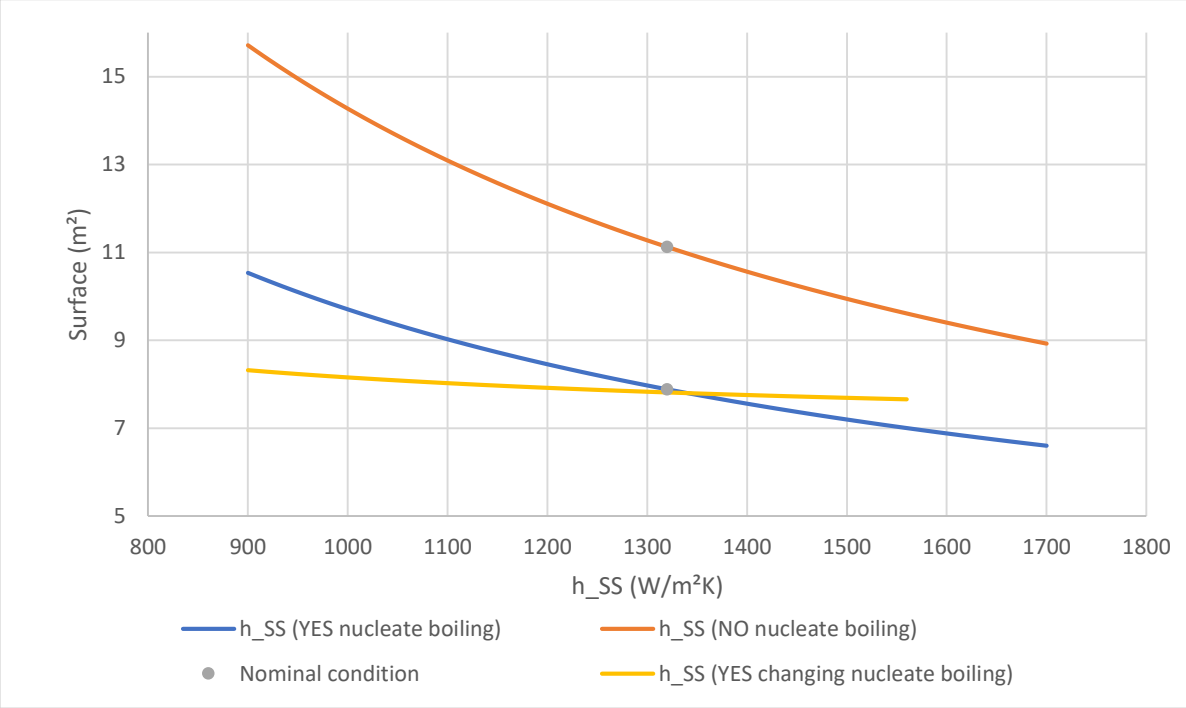

Figure 39: Secondary HTC's influence on the "liquid-liquid" PHE surface at FR=45%

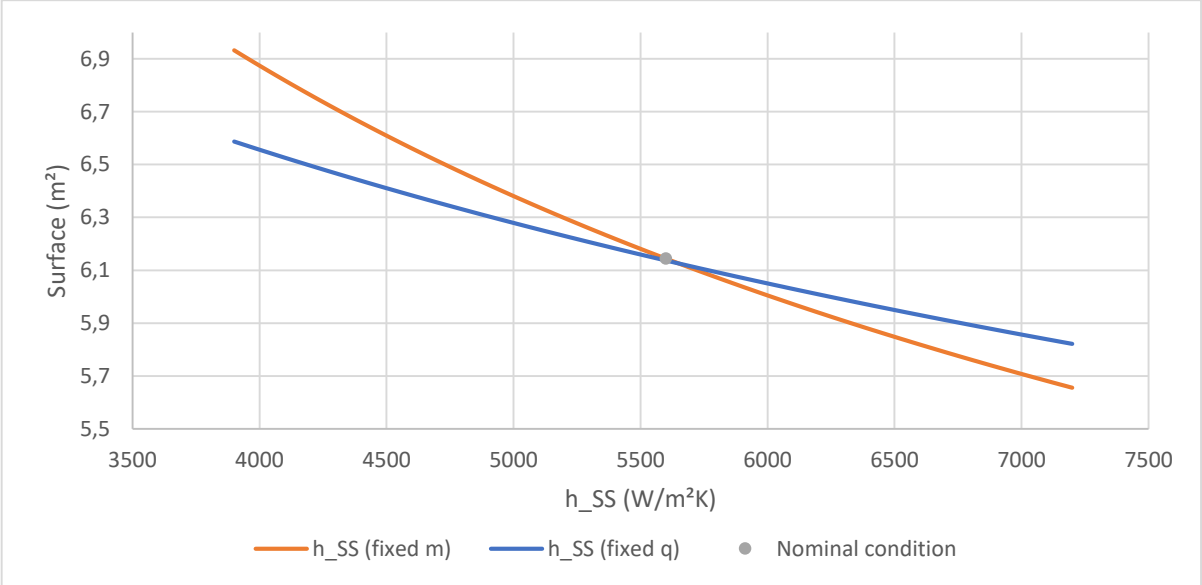

Figure 40: Secondary HTC's influence on the "liquid-evaporating" PHE surface at FR=45%. Both cases consider nucleate boiling occurring (q= $h_{1P_{SS}(ONB)}$, m= $h_{sat,vap}$)

Mass Flow Rate

As expected, a variation over the primary mass flow rate has a greater impact on the surface than the same variation of the secondary mass flow rate. After all, the former is always a five time greater than the ladder. Since the temperatures are fixed, an increase in mass flow rate translates in an increase of exchanged power, therefore a greater surface needed.

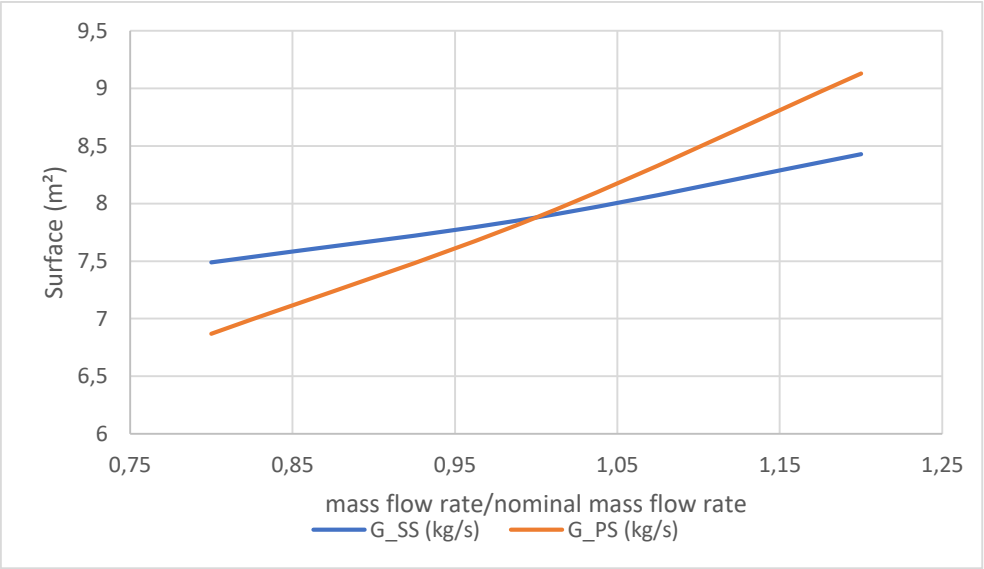

Figure 41: Primary and secondary mass flow rate influence on the "liquid-liquid" PHE surface at FR=45%

Moving on the liquid-evaporating side, a shift in trends occurs for the secondary side. This could be due to the presence of nucleate boiling on the secondary side, which increases the heat transfer coefficient, therefore less surface is needed in case of a mass flow rate increases (Figure 42).

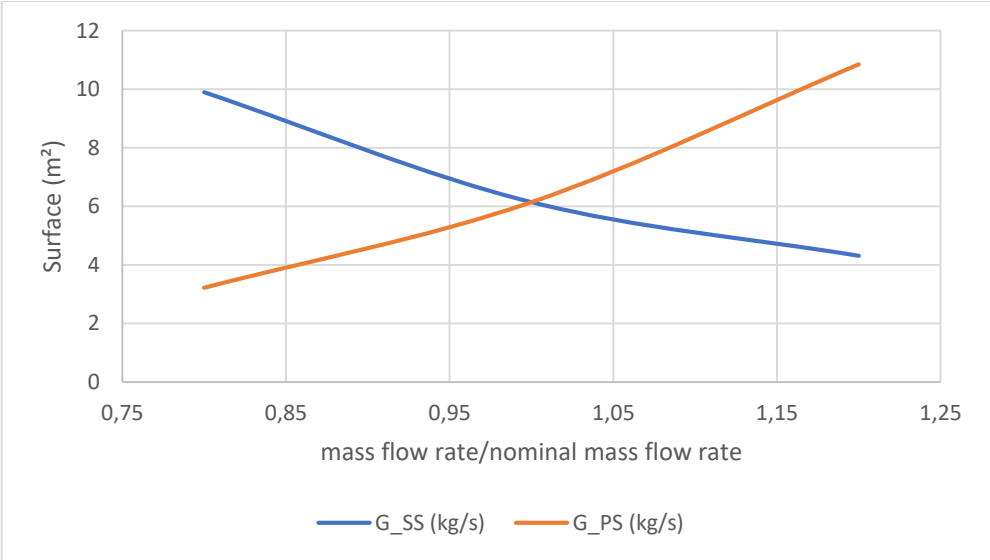

Figure 42: Primary and secondary mass flow rate influence on the "liquid-evaporating" PHE surface at FR=45%

Temperature

Primary and secondary temperature overall have a small influence on the heat transfer surface in the "liquid-liquid" part (Figure 43). On the other hand, when analyzing the "liquid-evaporating" part of the CSG, primary input temperature has a greater impact compared to other temperatures (Figure 44).

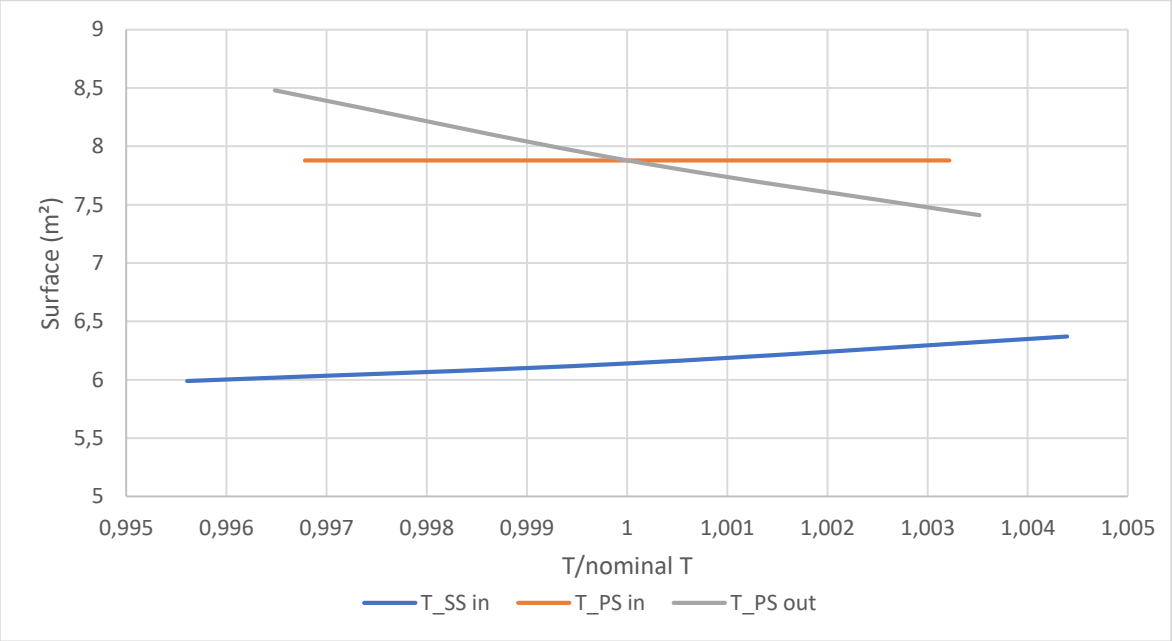

Figure 43: Temperature influence on the "liquid-liquid" PHE surface at FR=45%

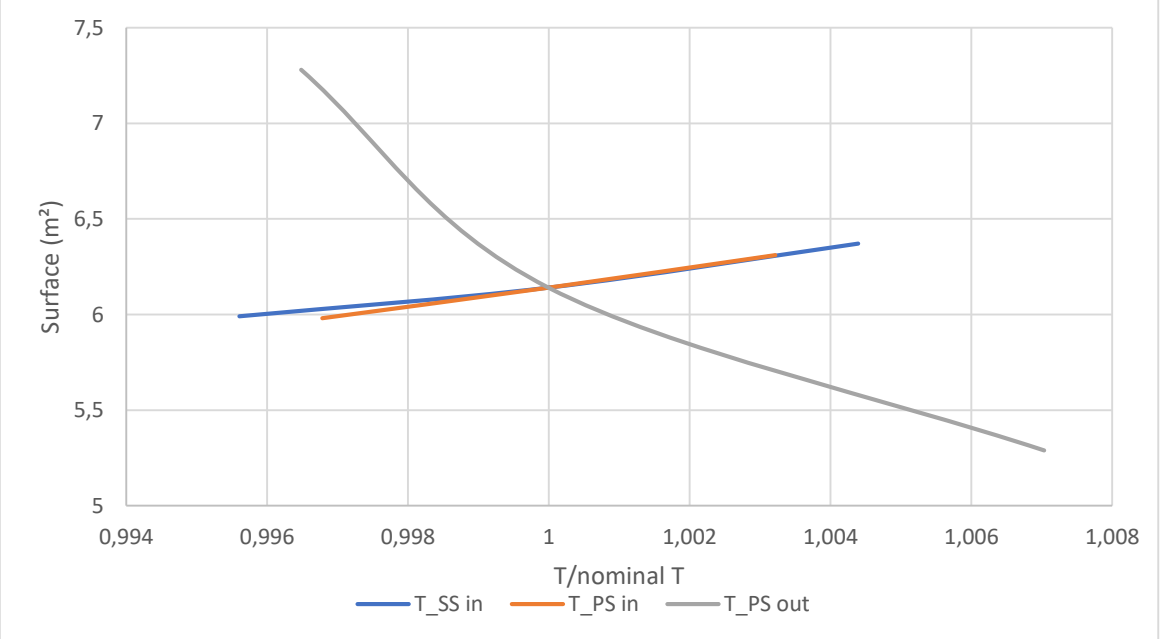

Figure 44: Temperature influence on the "liquid-evaporating" PHE surface at FR=45%

4 Conclusions and future developments

The strengths and disadvantages of SMR have been summarized, and the ELSMOR project and SIET experimental facility have been thoroughly explained. Together with the key findings, the significance of an experimental campaign is demonstrated. Using either a liquid-evaporating design or an evaporation-evaporating configuration, the ELSMOR facility's passive heat removal technology has proven effective under a variety of operational situations.

In order to characterize the heat transfer coefficient, first the overall heat transfer coefficient was calculated using the raw data gathered during the experimental campaign, and then this value was compared to the value predicted by the most accredited correlations in the literature. The most accurate estimate came from Muley & Manglick, which had a 24% error in its single-phase prediction of the total HTC. Correlations for the overall HTC for a mixed scenario (primary in single-phase and secondary in two-phase) were more inconsistent and heavily dependent on the particular data set; for instance, Heavner and Yan & Lin predicted with an error of only 2% (FR=17.44%) but were outperformed by other correlation combinations as soon as the data set was changed.

Finding a more accurate approach became necessary as discrepancies in the prediction models were shown. As a result, a semi-empirical correlation was built both on raw data and on the physical considerations by Amalfi et al and Solotych et al. However, because it overestimated the surface required by 100%, this correlation was unable to accurately predict on a test scenario like FR=45%. Its primary shortcomings were that it was trained on an inadequate amount of data and that it neglected to take into account processes like nucleate boiling.

The ad hoc correlation process was repeated once again. This time, it was derived by empirically fitting the data in order to attain the nominal heat transfer area rather than obtaining it from physical considerations and a literature review. Additionally, nucleate boiling has been pointed out as a justification for the improvement in heat transfer efficiency and subsequent decrease in surface need. With the help of the last approach, the error 15%. However, the little training data set is also here the key problem. Finally, a sensitivity analysis was performed on the main parameter impacting the heat transfer surface of the CSG at FR=45%.

In conclusion, because of the unique conditions under which the CSG operates, some literature correlations did not fit well because they mostly focused on a particular geometry (experimentally constructed PHE with few plates compared to industrial PHE with many plates), fluid (typically liquid water and R134a refrigerant compared to liquid water and steam), and operational conditions (R&D compared to industrial

applications). On the other hand, a deeper comprehension of the physical processes taking place within the CSG while it is operating could offer the required details for completely characterizing the heat thermal coefficient, particularly when operating in two-phase mode. As a result, it is suggested to launch an ad hoc experimental campaign that builds on the work begun in this thesis and involves an international effort from various universities and companies.

These types of PHE are cheap, readily available and easy to install compared to traditional steam generators for large reactors. Moreover, when employed as steam generators applied in the nuclear industry they represent, among other things, the final frontier that might ensure the proliferation of civil nuclear technology.

Bibliography

[1] European Commission, Directorate-General for Energy, "EU energy in figures : statistical pocketbook 2022," Publications Office of the European Union, 2022.

[2] EUROSTAT, Electricity production, consumption and market overview, 2023.

[3] NEA (2021), Small Modular Reactors: Challanges and Opportunities, Paris: OECD Publishing, 2021.

[4] IAEA (2020), Advances in Small Modular Reactor Technology Developments, A supplement to: IAEA Advances Reactors Information Systems (ARIS), IAEA, Vienna, 2020 Edition.

[5] "Periodic Reporting for period 2 - ELSMOR (Towards European Licencing of Small Modular Reactors)," 2022.

[6] ELSMOR, ELSMOR - About the project, 2022.

[7] Onda S.p.A., "Plate Heat Exchanger Working Principles," 2020. [Online].

[8] Ayub, "Plate Heat Exchanger Literature survey and New Heat Transfer and Pressure Drop correlations for Refrigerant Evaporator," *Heat Transfer Engineering,* 2003.

[9] R. Troupe, "The plate heater versatile chemical," *Chemical Engineering Progress 56,* pp. 124-128, 1960.

[10] W. Emerson, "The thermal and hydrodynamic performance of a plate heat exchanger: I and II," *National Engineering Laboratories,* 1967.

[11] T. Khan, "Experimental investigation of single phase convective heat transfer coefficient in a corrugated plate heat exchanger for multiple plate configurations," 2010.

[12] Muley&Manglik, "Experimental Study of Turbulent Flow Heat Transfer and Pressure Drop in a Plate Heat Exchanger With Chevron Plates," *ASME Journal of Heat and Mass Trasfer,* 1999.

[13] R. Heavner, Performance of an industrial heat exchanger: effect of chevron angle, in: AIChE Symposium Series No. 295, New York, 1993.

[14] H. Kumar, "The plate heat exchanger: construction and design," *The Institution of Chemical Engineers Symposium Series, Volume 2.86,* pp. 1275-1288, 1984.

[15] B. Thonon, "Design method for plate evaporators and condensers," *Mechanical Engineering Publications Limited,* pp. 37-50, 1995.

[16] Yan&Lin, "Condensation heat transfer and pressure drop of refrigerant R134a in a plate heat exchanger," *International Journal of Heat and Mass Transfer,* pp. 993-1006, 1999.

[17] Yan&Lin, "Evaporation Heat Transfer and Pressure Drop of Refrigerant R-134a in a Plate Heat Exchanger," *ASME, Journal of Heat and Mass Transfer,* pp. 118-127, Feb 1999.

[18] Khan, "Experimental investigation of evaporation heat transfer and pressure drop of ammonia in a 30° chevron plate heat exchanger," *International Journal of Refrigeration,* 2012.

[19] M. S. Khan, "Experimental investigation of evaporation heat transfer and pressure drop of ammonia in a 60° chevron plate heat exchanger," *International Journal of Refrigeration,* 2012.

[20] Park&Kim, "Evaporation heat transfer and pressure drop characteristics of R134a in the oblong shell and plate heat exchanger," *KSME International Journal,* 2004.

[21] E. Lee, "Flow boiling heat transfer and pressure drop of water in a plate heat exchanger with corrugated channels at low mass flux conditions," *International Journal of Heat and Mass Transfer,* 2014.

[22] R. L. Amalfi, "Flow boiling and frictional pressure gradients in plate heat exchangers. Part 1: Review and experimental database," *International Journal of refrigeration,* vol. 61, pp. 166-184, 2015.

[23] R. Amalfi, "Flow boiling and frictional pressure gradients in plate heat exchangers. Part 2: Comparison of literature methods to database and new

prediction methods," *International Journal of Refrigeration,* vol. 61, pp. 185-203, 2015.

[24] L. A. T. Valentin Solotych, "Boiling heat transfer and two-phase pressure drops within compact plate heat exchangers: Experiments and flow visualizations," *International Journal of Heat and Mass Transfer,* pp. 239-253, 2015.

A Appendix: Uncertainty analysis

Assessing the error in the model calculations is the purpose of the "uncertainty analysis." The scale of the model must be taken into account when interpreting the outcomes of the model calculations for management purposes, which is why the uncertainty analysis is crucial. Uncertainty analysis involves calculating an uncertainty distribution rather than a single value for each output variable and quantitatively measuring uncertainty in model components (input variables, parameters, and equations) for a specific situation.

The measurement uncertainty is evaluated according to the criteria and assumptions as described in the followings, on the basis of the UNI CEI ENV 13005 Standard and of the UNI CEI 70099 Standard. The measurement uncertainty includes many components. Some of these can be classified as Type A which uncertainty is evaluated by the statistical distribution of the quantity values coming from series of measurements. The other components are classified as Type B which measurement uncertainty evaluation is evaluated through probability density functions based on experience or other information. Errors presented in the calibration certificates and Errors declared by builders are included in this category. For the Type B uncertainty evaluation, a rectangular probability distribution has been assumed to be conservative. In fact, in the rectangular distribution, all the values in the range $\pm\, Error$ have the same probability of occurrence. The results of both the Type A and Type B uncertainty evaluation is a standard deviation. A coverage factor is chosen, $k = 2$, that represents the probability that the set of true values of the measured quantity is contained within the uncertainty range with a level of confidence of 95%.

The main input parameters into play are T and P. Mass flow rate, power and U are instead derived parameters whose uncertainty depend on various factors, including P and T. The T signal were measured with an RTD PT100 from Thermo Engineering (model RTD D=3 mm), while the P and differential P (DP) measurements were acquired with a relative P and DP transmitter from Honeywell (model STD870 and STD820). Knowing the instruments error and relative calibration uncertainty and the same for the acquisition system, it is straightforward to calculate the uncertainties related to T and P.

$$U_{tot} = U_{tot,\,instrument} + U_{tot,DAS} = \sqrt{\left(\frac{E_{instrument}}{\sqrt{3}}\right)^2 + \left(\frac{U_{instrument}}{2}\right)^2} + \sqrt{\left(\frac{E_{DAS}}{\sqrt{3}}\right)^2 + \left(\frac{U_{DAS}}{2}\right)^2}$$

where $\frac{1}{\sqrt{3}}$ is the rectangular probability distribution coefficient.

The mass flow rate's uncertainty was evaluated using the propagation of uncertainties rule:

$$U_F = 2 * \sqrt{\left(\frac{\partial F}{\partial \alpha}\right)^2 \cdot {U_\alpha}^2 + \left(\frac{\partial F}{\partial \varepsilon}\right)^2 \cdot {U_\varepsilon}^2 + \left(\frac{\partial F}{\partial d_H}\right)^2 \cdot {U_{d_H}}^2 + \left(\frac{\partial F}{\partial \rho}\right)^2 \cdot {U_\rho}^2 + \left(\frac{\partial F}{\partial DP}\right)^2 \cdot {U_{DP}}^2 + \left(\frac{\partial F}{\partial h}\right)^2 \cdot {U_h}^2}$$

Where the 2 in front of the square root is the coverage factor k that corresponds to a level of confidence of 95%. For vertically installed orifices, as in the case of the primary mass flow rate, there is also the contribution of the uncertainty U_h related to the manometrical line length.

For the power W and global heat transfer coefficient U, the procedure is equivalent:

$$U_W = 2 * \sqrt{\left(\frac{dW}{dF}\right)^2 * U_F^2 + \left(\frac{dW}{dcp}\right)^2 * U_{cp}^2 + \left(\frac{dW}{dTin}\right)^2 * U_{Tin}^2 + \left(\frac{dW}{dTout}\right)^2 * U_{Tout}^2}$$

$$U_U = 2 * \sqrt{\left(\frac{dU}{dQ}\right)^2 * U_Q^2 + \left(\frac{dU}{dA}\right)^2 * U_A^2 + \left(\frac{dU}{dLMTD}\right)^2 * U_{LMTD}^2}$$

List of Figures

List if Tables

List of symbols

Variable	Description	SI unit
c_p	Specific heat capacity	kJ/kg°C
d_e	Equivalent diameter	m
d_h	Hydraulic diameter	m
$\dot{m}$	Mass flow rate	kg/s
$1p$	Single phase	-
$2p$	Two phase	-
A	Heat transfer area	m²
b	Corrugation height	m
Bd	Bond number	-
Bo	Boiling number	-
G	Mass flux	kg/m²s
h	Heat transfer coefficient	W/m²K
k	Thermal conductivity	W/mK
Nu	Nusselt number	-
P	Pressure	MPa
Pr	Prandtl number	-
ps	Primary side	-
Re	Reynolds number	-
ss	Secondary side	-
T	Temperature	°C
t	Thickness of plate	m
U	Global heat transfer coefficient	W/m²K
W	CSG power	kW
We	Weber number	-
x	Vapor quality	-
β	Chevron angle	°
μ	Dynamic viscosity	Pa*s
σ	Surface tension	N/m
φ	Enlargement factor	-

List of acronyms

Acronym	Description
COST	Commercial Off the Shelf Components
CRDM	Control Rod Drive Mechanism
DAS	Data Acquisition System
EHRS	Emergency Heat Removal System
ELSMOR	European Licensing of Small Modular Reactors
ENRSREG	European Nuclear Safety Regulators Group
E-SMR	Experimental SMR
EURATOM	European Atomic Energy Community
FOAK	First Of A Kind
FR	Filling Ratio
HTC	Heat Transfer Coefficient
HVAC&R	Heating, Ventilation, Air-Conditioning, and Refrigeration
HX	Heat Exchanger
IAEA	International Atomic Energy Agency
KA-CARE	King Abdullah City for Atomic and Renewable Energy
KAERI	Korea Atomic Energy Research Institute
LOCA	Loss Of Coolant Accident
LR	Large Reactor
LRL	Licensing Readiness Level
LWR	Light Water Reactor
NEA	Nuclear Energy Agency
NSSS	Nuclear Steam Supply System
PHE	Plate Heat Exchanger
R&D	Research and Development
S-CSG	Safety Compact Steam Generator
SIET	Società Informazioni Esperienze Termoidrauliche
SMART	System Integrated Modular Advanced Reactor
SMR	Small Modular Reactor
TRL	Technology Readiness Level
VRE	Variable Renewable Energy
ONB	Onset of Nucleate Boiling

Acknowledgments

Particular thanks to the SIET personnel and my thesis advisor Roberta Ferri for allowing me this experience, for welcoming me on the team, and for supporting me through any difficulties I encountered while writing the thesis. thanks

Thanks to the Politecnico di Milano and to each and every professor who helped shape the student that I am today. I would especially want to thank Professors Ricotti and Lorenzi for their assistance with the composition of my master's thesis. Both were formerly my teachers, and I have the utmost respect for both.

I'm grateful for my family, who have always supported me and believed in my ability. They have never once discouraged me or treated me poorly because I was graduating later than usual.

Last but not least, thanks to my friends. Without them, I believe I would have never been able to complete my studies, particularly in the wake of the pandemic. I've been fortunate enough to have many friends throughout my life, but in the most recent years - the years that coincided with my master - two friend groups stood out for me in particular: "Serata Sium" and "Veterans." I've shared some of the most significant moments of my life with both of them in various occasions, and I will take care of those memories. Moments including organizing holidays, sharing a few beers, skiing, studying for exams together, chatting about the future, etc. In one way or another, they've all helped me find the drive to carry on with my academic endeavours.

I want to end this stream of consciousness with two quotes among some of my favourites. These were said from two of my favourite artist:

"If you have the opportunity to play this game called life, you have to appreciate every moment. A lot of people don't appreciate their moment until it's passed" - Kanye West

"They say you waste time asleep, but I'm just tryin' to dream" – Mac Miller from "Senior Skip Day"

Thank you.

Alessandro

P.S.

Everybody want to know what I would do if I didn't *graduate*... I guess we'll never know.